Our previous study showed that a Y-to-F substitution at the second position in Nef138-10 epitope (Nef138-2F) impairs the ability of the Nef138-10-specific CTLs to suppress HIV-1 replication, indicating that Nef138-2F is an escape mutation from CTLs [23]. Since Nef138-2F is observed in both HLA-A*2402-positive and -negative patients, Nef138-2F variant may be stable and adopted at a population level [21].

In the present study of early antiretroviral treatment with five series of STIs for HLA-A *2402 positive Japanese patients, we investigated the longitudinal magnitudes of HIV-1-specific HLA-A*2402-restricted CTLs by using HLA-epitope tetramer binding assay and sequenced the most immunodominant epitopes Nef138-10 to evaluate whether escape mutation might negatively influence viral control in an STI study.

2. Methods

2.1. Study design and patient population

This trial was designed as a prospective study at the AIDS Clinical Center, International Medical Center of Japan. Between November 2000 and December 2001, patients with early HIV infection, with or without acute retroviral symptoms, were recruited. Early HIV infection was confirmed within 6 months before recruitment by a documented history of seroconversion in enzyme-linked immunosorbent assay (ELISA) or longitudinal increase of bands in Western blot test. Patients with active opportunistic infections or psychological disorders, or those treated with immunomodulatory agents were excluded. Antiretroviral therapy was initiated after obtaining a signed informed consent. The first-choice regimen for this study consisted of stavudine, lamivudine and indinavir boosted with ritonavir, but the patient was allowed to use other antiretroviral drugs when the first regimen could not be tolerated. To avoid emergence of drug resistance to indinavir, ritonavir-boosting was stopped more than 1 week before treatment interruption. The duration of treatment interruption was fixed for 3 weeks. The first treatment was interrupted after more than 3 months of HAART, when CD4+ cell count was $>500/mm^3$ and plasma viral load (pVL) had been <50 copies/ml for at least 1 month. Other interruptions were also carried out when pVL became <50 copies/ml and CD4+ cell count was $>300/mm^3$. Five series of STIs were scheduled during the treatment.

The study protocol was approved by the institutional ethical review boards (IMCJ-H13-10).

2.2. Monitoring and sample collection

Patients were monitored monthly during HAART and at approximately a 4-month interval after treatment discontinuation. Unscheduled visits were permitted according to clinical needs. At each visit, clinical assessment and routine laboratory tests were performed. Blood specimens were collected in ethylenediaminetetraacetic acid (EDTA)-containing tubes, separated into peripheral blood mononuclear cells (PBMCs) and plasma, and stored at −80 °C for assessment of HIV-1-specific CTLs and sequence of the dominant epitope region. pVL was quantified by using the Amplicor HIV-1 Monitor test 1.5 (Roche Diagnostics, Indianapolis, IN) with a detection limit of 50 copies/ml. Antiretroviral drug resistance-associated mutations were examined at baseline and after HAART including STIs in all 26 participants. Each mutation was identified according to the revised August 2006 International AIDS Society Resistance-USA Panel [24].

2.3. HLA typing and epitope-HLA-A*2402 tetramer binding assays

High-resolution HLA class I typing was performed by a PCR-sequence-specific primer method. If HLA-A*2404 was positive, HIV-1 specific CTLs were investigated by using peptide-HLA-A*2402 tetrameric complex synthesized as described previously [21,22,25]. Purified complexes were enzymatically biotinylated at a BirA recognition sequence located at the C-terminus of the heavy chain, and then mixed with phycoerythrin (PE)-conjugated avidin (extravidin-PE; Sigma–Aldrich, St. Louis, MO) at a molar ratio of 4:1. Cryopreserved PBMCs ($0.5-1 \times 10^6$ cells) were stained by the tetramer at 37 °C for 30 min. After double washing with washing buffer (10% fetal calf serum in RPMI 1640), the cells were stained by fluorescein isothiocyanate (FITC)-conjugated anti-human CD8 mAb (BD Biosciences, San Jose, CA) at 4 °C for 30 min. The cells were then washed twice and analyzed using a FACS Calibur with Cell Quest software (Becton Dickinson, San Jose, CA). Based on our previous study [22], three immunodominant epitopes of HLA-A*2402 restricted CTLs; Nef138-10, Gag28-9 and Env584-9, were chosen for this assay. Since we found a high frequency of Y-to-F substitution at the second position in Nef138-10 gene (Nef138-2F) which has been suspected as an escape variant in previous studies [21], Nef138-2F-specific CTLs (Nef138-2F-CTLs) were also measured by tetramers using Nef138-2F variant alone and by competitive double staining using two types of tetramers of both wild type and Nef138-2F variant to compare the frequencies of the two types of HIV-1-specific CTLs.

2.4. Sequence analyses of Nef138-10 gene

For evaluation of escape variants from CTLs, we sequenced the region coding Nef138-10, which is the immunodominant HLA-A*2402-restricted epitope, while Nef138-2F has been suspected as escape mutation in this epitope, using the method described here. Total RNA was extracted from plasma with a High Pure viral RNA kit (Boehringer Mannheim, Mannheim, Germany), followed by RT–PCR with a One Step RNA PCR kit (TaKaRa Shuzo, Otsu, Japan) to amplify the HIV-1 Nef DNA segment (2341 bp) as described previously [21]. The PCR products were purified with SUPREC-02 (TaKaRa Shuzo) and subjected to direct sequencing with an ABI PRISM 3730 automated DNA sequencer (Applied Biosystems, Foster City, CA). Amino acid sequences were deduced with the Genetyx-Win program version 5.1 (Software Development, Tokyo).

2.5. Statistical analysis

Data from patients who completed the treatment protocol including five series of STIs were analyzed. Before analysis, pVL data were log-transformed and undetectable pVL (<50 copies/ml) was considered equivalent to 50 copies/ml. The Mann–Whitney *U*-test was used to compare the pVLs determined every 3 months after treatment cessation to the pVLs of 279 untreated chronic HIV-1 patients in order to assess the durability of viral suppression. The correlation between pVL and percentage of CTLs was assessed by simple regression analysis. Statistical analyses were performed using SPSSII software package for Windows, version 11.0J.

3. Results

3.1. Characteristics of participants

During the enrollment period, 432 new patients were referred to our clinic. Of these, 32 met the criteria of early HIV-1 infection and 6 were excluded due to psychological problems or taking systemic steroid therapy for symptoms associated with acute retroviral syndrome. All 26 recruits were Japanese infected with HIV-1 by sexual intercourse, and 24 were men (92%). The mean age of patients was 35.0 years (range, 21–56 years). The mean pVL at baseline was 5.21 $\log_{10}$ copies/ml (range, 3.28–6.91 $\log_{10}$ copies/ml) and the mean CD4+ cell count at baseline was 413/mm^3 (range, 49–1156/mm^3). Twenty-five patients presented with wide-range clinical symptoms of acute retroviral syndrome. Fifteen out of 26 participants completed the treatment protocol including five series of STI. HAART had to be continued in four patients because CD4+ cell counts had never stabilized above 300/mm^3 despite more than 6 months of treatment. The other seven patients discontinued the treatment protocol after less than five STIs due to adverse events, adherence problems, or no specific problems.

In the protocol-completed 15 patients, 14 were men (92%). The mean age was 34.0 years (range, 21–56 years). At baseline, the median pVL was 5.14 $\log_{10}$ copies/ml (range, 3.28–6.91 $\log_{10}$ copies/ml) and the median CD4+ cell count was 475/mm^3 (range, 245–990/mm^3). The demographic, immunological, and virological factors before initiation of HAART of the protocol-completed group were not statistically different from those of the uncompleted group (Mann–Whitney *U*-test) (data not shown), although baseline CD4+ cell counts of four ART-continued patients: 49, 185, 210, and 351/mm^3 respectively seemed lower than those who completed the treatment protocol. Twelve (80%) patients were positive for HLA-A*2402 and its incidence was similar to those reported previously in Japanese population [21,22]. No specific HLA genotypes that are known to influence the clinical course of HIV infection such as HLA-B*27, HLA-B*57 and HLA-B*35 (except B*3501) [26] were detected in participants. The median length of follow-up after treatment cessation was 961 days (range, 462–1255 days).

No resistance-associated mutations were identified among all the 26 participants at study enrollment except one who had M184V, D30N and L90M mutations despite good virologic responses throughout HAART. There was no increase in resistance-associated mutations during and after five STIs in all participants (data not shown).

3.2. Plasma viral load and CD4+ cell count in protocol-completed 15 patients

Fig. 1 shows serial changes in median pVLs and CD4+ cell counts in protocol-completed 15 patients. Peaks of viral

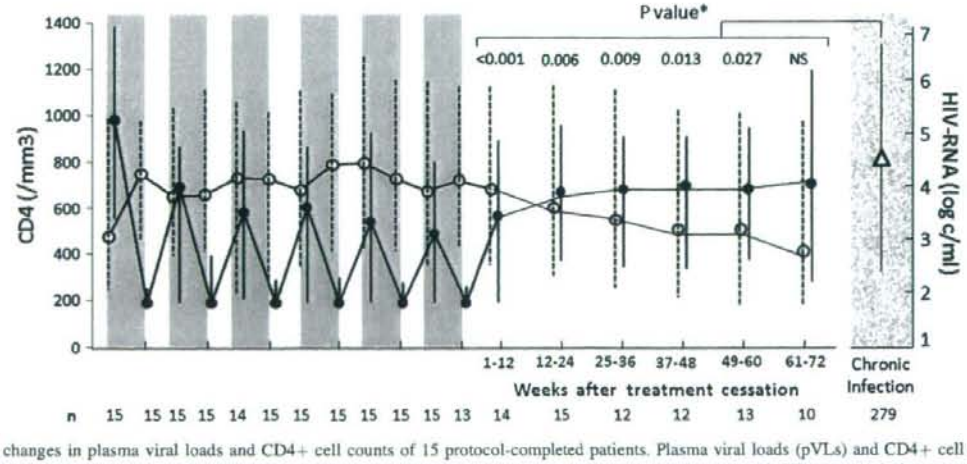

Fig. 1. Serial changes in plasma viral loads and CD4+ cell counts of 15 protocol-completed patients. Plasma viral loads (pVLs) and CD4+ cell counts are expressed as median of 15 protocol-completed patients; at baseline, at the times of treatment interruption, at the peaks of pVL rebound during structured treatment interruption and at every 12 weeks after treatment cessation. Open circles: CD4+ cell counts; solid circles: pVLs; triangle: the median pVL of 279 untreated chronic HIV-1 patients who were referred to our clinic during the study and whose CD4 count was >200/mm^3. Vertical lines provide the ranges with dotted lines in CD4+ cell counts and with light lines in pVLs. Shaded area: time on antiretroviral therapy; unshaded area: time off therapy. Numbers of patients whose data were evaluated at each time point appear at the bottom of the graph. *pVLs of every 12 weeks after treatment cessation were compared to the pVLs of 279 untreated chronic HIV-1 patients by Mann–Whitney *U*-test.

rebounds during treatment interruptions decreased gradually. The pVLs of every 12 weeks after treatment cessation were under 4 $\log_{10}$ copies/ml in most of the patients and they were significantly lower for 60 weeks than the pVLs of 279 untreated chronic HIV-1 patients in our clinic. However, pVLs gradually increased and there was no difference at week 61–72 from pVLs of chronically infected patients. The proportion of patients with a favorable viral control whose median pVL at every 12 weeks after treatment cessation were less than 4.0 $\log_{10}$ copies/ml was 66% in the first 12 weeks but the proportion decreased to 33% in the 61–72 weeks. Along with the increase in pVL, CD4+ cell counts declined after treatment cessation and one patient (KI-134) required restart of HAART because CD4+ cell count decreased below 200/mm^3 at week 52. None of the patients developed episode of opportunistic infections or HIV-related diseases throughout this study.

*3.3. Plasma viral loads and frequency of HLA-A*2402-restricted CTLs*

We investigated induction of 3 HLA-A*2402-restricted immunodominant epitope-specific CTLs in 12 patients with HLA-A*2402 by using the corresponding tetramers. Fig. 2 shows the serial changes in HLA-A*2402-restricted HIV-1-specific CTLs. Overall, the frequency of HLA-A*2402-restricted CTLs varied widely among the patients and a sustained CTL response was rarely noted. We investigated the correlation between pVLs at every 12 weeks after treatment cessation and frequency of HLA-A*2402-restricted CTLs according to the epitope. None of Nef138-10-, Gag28-9- or Env584-9-specific CTLs was statistically correlated to pVLs (Fig. 3A).

3.4. Effect of Nef138-10 escape mutation on suppression of HIV replication

A Y-to-F substitution at the second position of Nef138-10 (Nef138-2F) has been suspected as an escape mutation from HLA-A*2402-restricted Nef138-10-specific CTLs in a previous study [21]. In fact, we recently demonstrated that Nef138-10-specific CTLs fail to suppress replication of Nef138-2F mutant [23]. We therefore performed serial sequence analyses of Nef138-10 epitope and investigated whether this 2F mutation is responsible for the limited duration of viral suppression. As shown in Table 1, we found high frequency of this mutation. Seven out of 12 patients had Nef138-2F variant in viral RNA or proviral DNA in the earliest samples (KI-091, KI-126, KI-134, KI-144, KI-150, KI-154 and KI-163). The Nef138-2F variant was not detected in the earliest samples of the other five patients (KI-092, KI-099, KI-102, KI-158 and KI-161) and these patients were considered to have Nef138-10 wild-type infection except a T-to-C substitution at the fifth position (Nef138-5C) in KI-099 which has also been suspected as one of the escape variants from Nef138-10-specific CTLs in a previous study [21], and an L-to-I substitution at the forth position (Nef138-4I) in KI-161. However, Nef138-2F mutation was detected at the latter stage in all the other five patients.

We speculated that Nef138-10-specific CTLs can control replication of HIV-1 in patients who had been infected with Nef138-WT virus. Therefore we compared pVLs according to the existence of escape mutants Nef138-2F or 138-5C at the earliest sample drawn during early phase of infection before treatment initiation. As shown in Fig. 3B, the pVLs between 13 and 36 weeks were significantly lower in the other four patients who were confirmed as Nef138-WT or Nef138-4I infection than in the remaining eight patients who had Nef138-2F or Nef138-5C variant in the earliest samples, which has been suspected as an escape variant from Nef138-10-specific CTLs in a previous study. These indicate that Nef138-10-specific CTLs control replication of wild-type virus but the presence of either Nef138-2F or Nef138-5C negatively influences viral control.

3.5. Nef138-2F variant specific CTLs

We found Nef138-WT-tetramer and Nef138-2F-tetramer bound to both Nef138-WT-specific CTL clones and Nef138-2F-specific CTL clones. In addition, Nef138-WT-tetramer had stronger affinity to Nef138-WT-specific CTL clones than Nef138-2F-specific CTL clones (Fig. 4A) and vice versa (our unpublished work). Therefore, the double-staining assay using both tetramers simultaneously was performed to differentiate the two types of CTLs.

The frequencies of the two types of CTLs are shown in Table 1. In patients negative for Nef138-2F or Nef138-5C initially, Nef138-WT-CTLs were detected early after the treatment cessation (KI-092, KI-102, KI-158 and KI-161) but declined after evolution of Nef138-2F (KI-092, KI-102, and KI-161). Although only a slight elevation of Nef138-2F-CTLs was noted after emergence of Nef138-2F (KI-092 and KI-161), the magnitude was smaller than that of Nef138-WT-specific CTLs before emergence of Nef138-2F.

In patients having Nef138-2F variant initially and suspected as Nef138-2F variant infection, the frequencies of Nef138-2F-CTLs were relatively smaller than those of Nef138-WT-specific CTLs in Nef138-10 wild-type infection, except KI-144 who had marked increase of Nef138-2F-CTLs in week 37.

Fig. 4B and C illustrate the clinical courses of two representative cases; KI-161 was non-Nef138-2F variant infection and KI-144 was suspected as Nef138-2F variant infection. In KI-161 (Fig. 4B), Nef138-WT-CTL response diminished after the emergence of Nef138-2F mutation. Interestingly, the pVL of this patient seemed to increase along with the fall in Nef138-WT-CTLs (Fig. 2). In KI-144 (Fig. 4C), Nef138-2F-CTLs were induced but there was no suppression of pVLs. These results indicate that either infection or emergence of Nef138-2F variant might limit the CTL induction.

4. Discussion

In this study, we could not demonstrate the lowered set-point pVLs in patients who received HAART with five series of STIs in early HIV-1 infection. Previous studies revealed that a vigorous HIV-1-specific CD4 response is associated

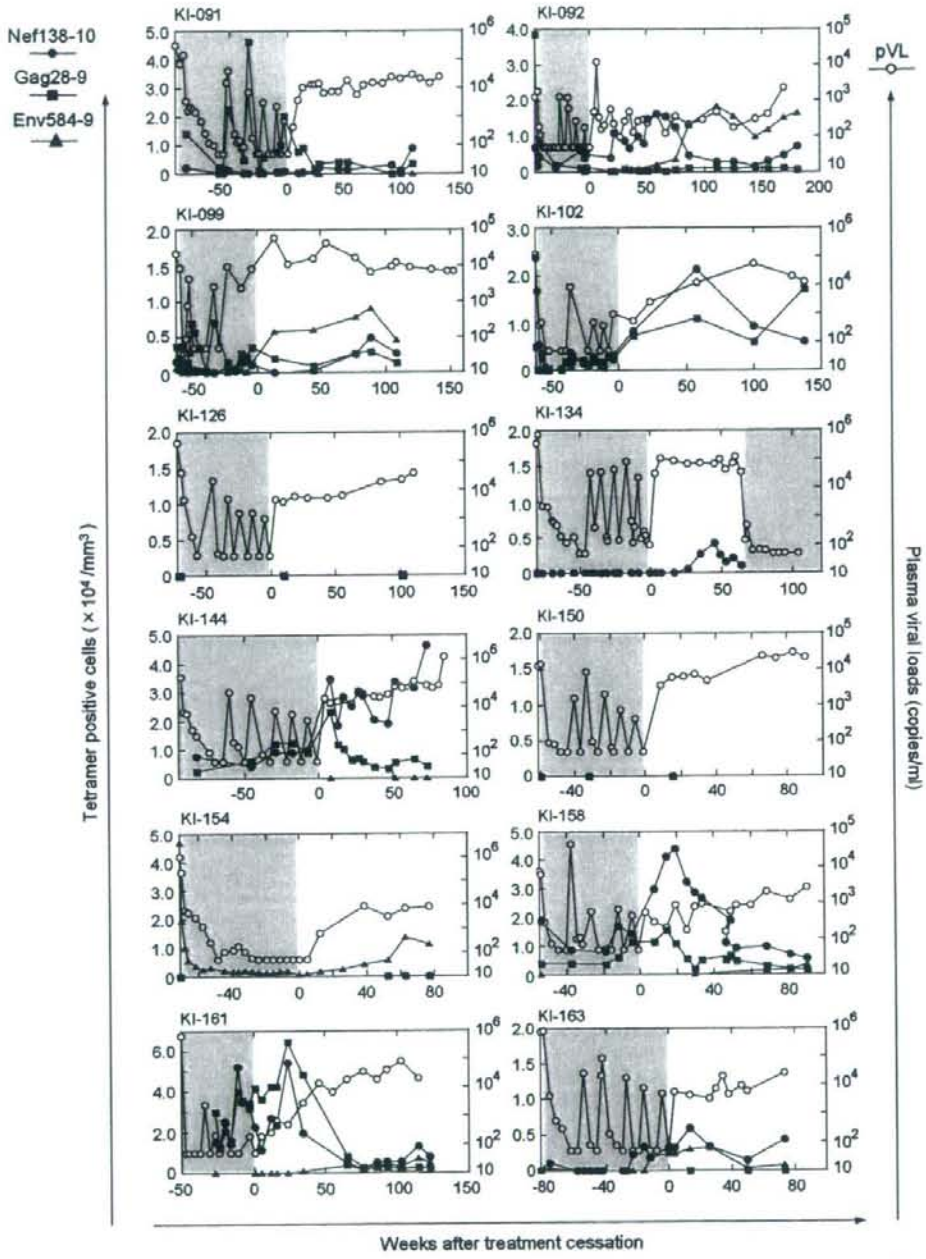

Fig. 2. Frequencies of HLA-A*2402 restricted HIV-1-specific CTLs determined by tetramer binding assay. HLA-A*2402 restricted HIV-1-specific CTLs in PBMCs were determined by using tetrameric complexes of HLA-A*2404 and each of the three types of epitopes. Solid circle: Nef138-10-specific CTL; solid squares: Gag28-9-specific CTL; solid triangles: Env584-9-specific CTL; open circles: plasma viral load. Shaded area: time on antiretroviral therapy; unshaded area: time off therapy.

with a slower disease progression [8–11]; however, despite some reports of boosted immunological responses in acutely treated patients, the evidence of clinical benefits of early treatment has not been established [12,13]. In line with these trials of early initiation of HAART with or without STI, the CTL responses in our study were mostly transient and did not correlate with pVL levels.

We adopted HLA-epitope tetramer analysis for evaluating CTL responses, which provides specific information on HLA class I allele and HLA-restricted epitopes, because CTL

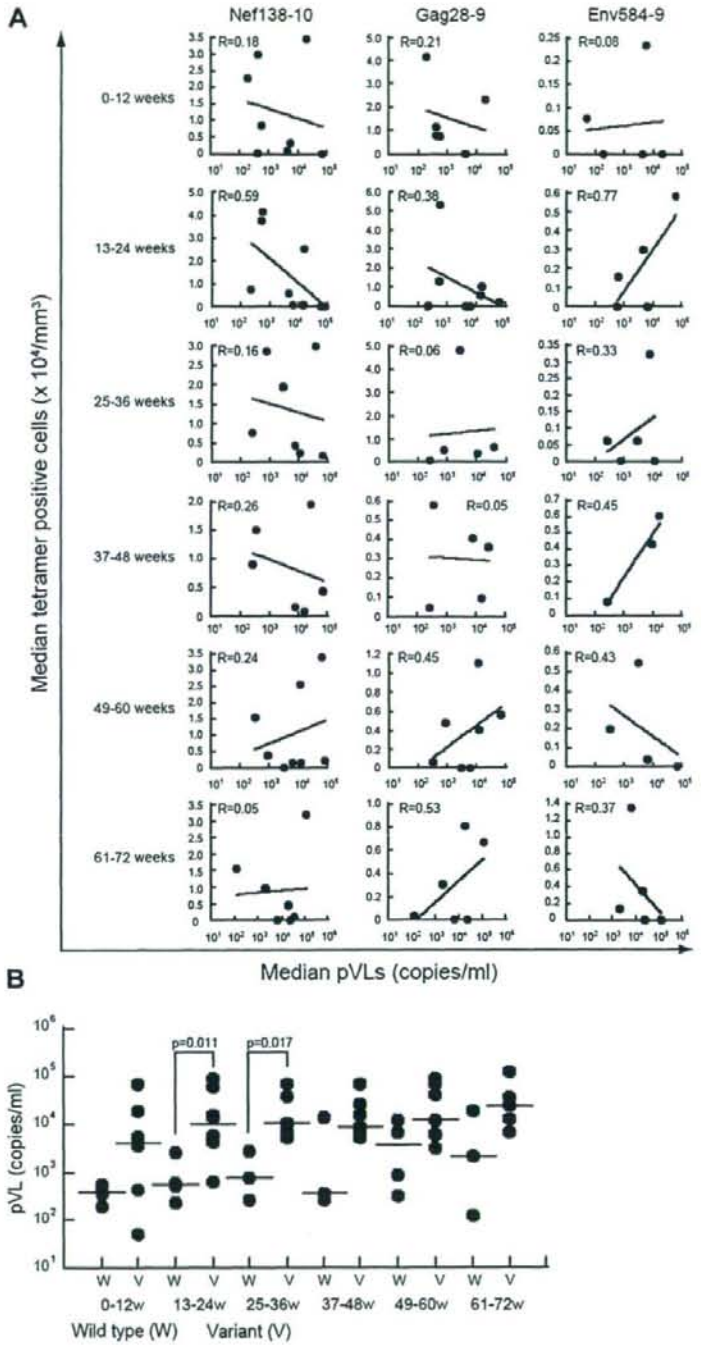

Fig. 3. (A) Plasma viral loads and frequency of HLA-A*2402-restricted HIV-1-specific CTLs. The correlation between the pVL values of every 12 weeks after treatment cessation and frequency of HLA-A*2402-restricted CTLs was assessed by simple regression analysis according to the epitope in 12 HLA*A2402-positive patients. None of Nef138-10-, Gag28-9- or Env584-9-specific CTLs was statistically correlated to pVLs at any time point. R: correlation coefficient. (B) Plasma viral loads and initial type of virus. pVL was compared according to the existence of escape variant in the earliest sample drawn during early phase of infection. Wild type group (W) includes four patients: KI-092, KI-102, KI-158 and KI-161. Variant type group (V) includes eight patients: KI-091, KI-099, KI-126, KI-134, KI-144, KI-150, KI-154 and KI-163, having Nef138-2F or Nef138-5C, which were previously reported as escape variants, in viral RNA or proviral DNA in the earliest samples. The pVLs between 12 and 36 weeks were significantly higher in Variant type group than in Wild-type group. Horizontal lines: median values.

Table 1
Nef138-10 sequence and Nef138-specific CTLs in HLA-A*2402 positive patients

Patient ID	Time (weeks)[a]	Sample	Nef138-10 sequence (RYPLTFGWCF)	Tetramer positive cell (% in CD8+ cells)	
				Wild type	2F
KI-091	−55	Proviral DNA	-F————	NA	NA
	21	RNA	-F————	0	0.46
	89	RNA	-F————	0	0.83
KI-092	39	RNA	————	1.48	0.05
	86	RNA	-F————	0.41	0.13
KI-099	−44	Proviral DNA	——C———	NA	NA
	−4	RNA	-F–C————	0.04	0.06
	44	RNA	-F————	0.02	0.12
KI-102	58	RNA	————	2.11	0.45
	137	RNA	-F————	0.45	0.10
KI-126	−68	Proviral DNA	-F————	NA	NA
	19	RNA	-F————	0.01	0.06
	101	NA	NA	0	0.11
KI-134	9	Proviral DNA	-F————	NA	NA
	49	RNA	-F————	0	0.22
KI-144	−46	Proviral DNA	-F————	NA	NA
	37	RNA	-F————	0.02	2.45
	71	RNA	-F————	NA	NA
KI-150	−43	RNA	-F————	NA	NA
	21	RNA	-F————	0	0.03
	63	NA	NA	0	0.02
KI-154	−70	Proviral DNA	-F————	0.06	0.13
	77	RNA	-F————	0.01	0.35
KI-158	14	Proviral DNA	————	2.91	0.41
KI-161	−26	Proviral DNA	—I————	NA	NA
		RNA	-F-I————		
	24	Proviral DNA	-F-I————	3.94	0.05
		RNA	-F-I————		
	86	Proviral DNA	-F-I————	0.29	0.79
		RNA	-F-I————		
	52	RNA	-F————	0.71	0.66
KI-163	−81	Proviral DNA	-F————	NA	NA
		RNA	-F————		
	26	RNA	-F————	0.09	0.57
	73	NA	NA	0.02	0.59

[a] Time: Time in weeks after treatment cessation. Negative time numbers: before treatment cessation. NA, not available.

responses are different between HLA class I alleles and influenced by viral mutations in epitope regions as described elsewhere [16–22]. HLA-A*2402 is the most frequent HLA class I allele with 70% prevalence in the Japanese population [21,22]. Therefore, the majority of the study participants could be assessed by using HLA-A*2402-epitope tetramer and thus it is most beneficial to evaluate HLA-A*2402 restricted CTL responses for Japanese patients. Moreover, HLA-A*2402-restricted epitopes have been studied extensively [22] and we were able to focus on three immunodominant epitopes. This approach allowed us to find a high frequency of the escape variant Nef138-2F efficiently.

Viral mutation is one of the important mechanisms of immune escape of HIV-1 [16–23,27–29], which occurs at amino acids responsible for HLA binding, T-cell receptor recognition, or in flanking regions that affect antigen presentation. In our study Nef138-2F, which is a mutation in the immunodominant CTL epitope Nef138-10, had emerged in 5 of 12 HLA-A*2402-positive patients. Although the magnitude of Nef138-10-specific CTLs was not significantly correlated with pVLs as previous trials [15], Nef138-2F variant infection was correlated with high pVL levels in early clinical course and seemed to contribute to lower CTL response. Furthermore, we previously demonstrated the strong and weak ability of Nef138-10-specific CTL clones to suppress replication of the wild-type and 2F mutant viruses respectively [23]. In addition, although Nef138-2F-specific CTL clones suppressed the replication of both wild-type and Nef138-2F variant, their ability to suppress the replication of Nef138-2F virus was much weaker than that of Nef138-10-specific CTLs or Nef138-2F-specific CTLs against the wild-type virus replication. Furthermore, the present study demonstrated that 2F mutant appeared at the late phase in patients who had wild-type virus at the early phase. Together with these findings, frequent detection of Nef138-2F in this study strongly supports the idea that Nef138-2F is one of the escape mutations from HLA-A*2402-restricted CTLs and that Nef138-2F virus was selected by CTL pressure.

Nef138-2F mutation could occur not only by positive selection by CTLs but also by Nef138-2F-variant transmission [19–21]. Furutsuki et al. [21] reported frequent detection of

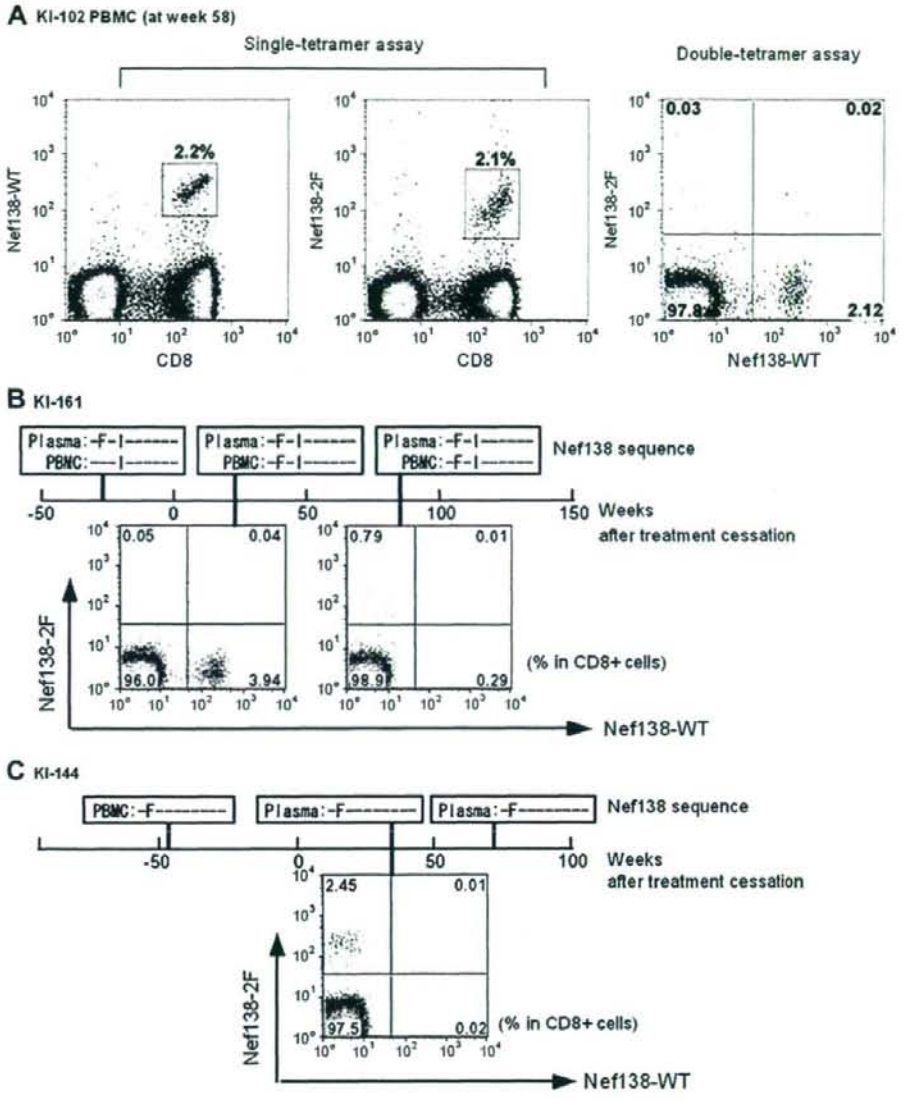

Fig. 4. Nef138-2F variant and CTL specificity. (A) PBMC of KI-102 at week 58, known to coincide with Nef138-10 wild-type infection, were assayed for wild-type Nef138-10-specific CTL (Nef138-WT-CTL) by tetramer-staining with Nef138-WT-tetramer and Nef138-2F-tetramer. The left two charts depict the results of single-tetramer-staining, showing the two tetramers stained for Nef138-WT-CTL equally (2.2% by Nef138-WT-tetramer versus 2.1% by Nef138-2F-tetramer). The right chart depicts the result of double-tetramer-staining with Nef138-WT-tetramer and Nef138-2F-tetramer, showing Nef138-WT-CTL was stained by Nef138-WT-tetramer and was differentiated from Nef138-2F-CTL. (B) Serial changes in Nef138-10 sequence and Nef138-specific-CTLs of KI-161 infected by non-Nef138-2F strain. Top: the Nef138-10 sequence; bottom charts: results of double-staining assay with Nef138-WT-tetramer and Nef138-2F-tetramer. Numbers in each quadrant represent the frequency of tetramer-positive cells among total CD8+ cells. Right lower quadrant: frequency of Nef138-WT-tetramer-positive cells; left upper quadrant: frequency of Nef138-2F-tetramer-positive cells. Note the induction of Nef138-WT-CTL and reduction in their proportion after emergence of Nef138-2F mutation. Nef138-2F-CTLs were induced after emergence of Nef138-2F mutation but their proportion was relatively lower. (C) Serial changes in Nef138-10 sequence and Nef138-specific-CTLs of KI-144 infected by Nef138-2F variant. Note the induction of Nef138-2F-CTL. Nef138-WT-CTLs were never detected throughout the study.

Nef138-2F variant in HLA-A*2402 negative Japanese patients who were infected by sexual intercourse and reversion from Nef138-2F to wild type occurred very slowly over years. These might allow horizontal spread of Nef138-2F variant. Even if the transmission of this variant in Japanese patients is very frequent, our study included the five patients who did not have this variant initially and were considered as wild-type infection, and we provided longitudinal evidence of positive selection of Nef138-2F variant under the pressure of Nef138-WT-CTLs in those.

In conclusion, our study demonstrated that early antiretroviral treatment with five series of STI did not induce a sustained immune response. A high frequency of escape mutation in the immunodominant HLA-A*2402-restricted CTLs was found, which could be one of the causes of limited immune responses by STIs.

Acknowledgments

We thank Manami Satoh and Hirokazu Koizumi (Division of Viral Immunology, Center for AIDS research, Kumamoto University), for assistance in epitope-HLA tetramer assay. No conflicts of interest declared by all authors. This work was supported by grants for AIDS research from the Ministry of Health, Labor, and Welfare of Japan (AIDS-H15-001).

References

[1] J. Lisziewicz, E.S. Rosenberg, J. Lieberman, J. Heiko, L. Lopalco, R. Siliciano, B. Walker, F. Lori, Control of HIV despite the discontinuation of antiretroviral therapy, N. Engl. J. Med. 340 (1999) 1683–1684.

[2] E.S. Rosenberg, M. Altfeld, S.H. Poon, M.N. Phillips, B.M. Wilkies, R.L. Eldridge, G.K. Robbins, R.T. D'Aquila, P.J.R. Goulder, B.D. Walker, Immune control of HIV-1 after early treatment of acute infection, Nature 407 (2000) 523–526.

[3] F. Lori, M.G. Lewis, J. Xu, G. Varga, D.E. Zinn Jr., C. Crabbs, W. Wagner, J. Greenhouse, P. Silvera, J. Yalley-Ogunro, C. Tinelli, J. Lisziewicz, Control of SIV rebound through structured treatment interruptions during early infection, Science 290 (2000) 1591–1593.

[4] J. Lawrence, D.L. Mayers, K.H. Hullsiek, G. Collins, D.I. Abrams, R.B. Reisler, L.R. Crane, B.S. Schmetter, T.J. Dionne, J.M. Saldanha, M.C. Jones, J.D. Baxter, Structured treatment interruption in patients with multidrug-resistant human immunodeficiency virus, N. Engl. J. Med. 349 (2003) 837–846.

[5] A. Lafeuillade, C. Poggi, G. Hittinger, E. Counillon, D. Emilie, Predictors of plasma human immunodeficiency virus type 1 RNA control after discontinuation of highly active antiretroviral therapy initiated at acute infection combined with structured treatment interruptions and immune-based therapies, J. Infect. Dis. 188 (2003) 1426–1432.

[6] M. Plana, F. Garcia, A. Oxenius, G.M. Ortiz, A. Lopez, A. Cruceta, G. Mestre, E. Fumero, C. Fagard, M.A. Sambeat, F. Segura, J.M. Miro, M. Arnedo, L. Lopalcos, T. Pumarola, B. Hirschel, R.E. Phillips, D.F. Nixon, T. Gallant, J.M. Gatell, Relevance of HIV-1-specific CD4+helper T-cell responses during structured treatment interruptions in patients with CD4+T-cell nadir above 400/mm^3, J. Acquir. Immune. Defic. Syndr. 36 (2004) 791–799.

[7] B. Hoen, I. Fournier, C. Lacabaratz, M. Burgard, I. Charreau, M.L. Chaix, J.M. Molina, J.M. Livrozet, A. Venet, F. Raffi, J.P. Aboulker, C. Rouzioux, Structured treatment interruptions in primary HIV-1 infection. The ANRS 100 PRIMSTOP Trial, J. Acquir. Immune. Defic. Syndr. 40 (2005) 307–316.

[8] P. Borrow, H. Lelicki, B.H. Hahn, G.M. Shaw, M.B.A. Oldstone, Virus-specific CD8$^+$ cytotoxic T-lymphocyte activity associated with control of viremia in primary human immunodeficiency virus type 1 infection, J. Virol. 68 (1994) 6103–6110.

[9] G.S. Ogg, X. Jin, S. Bonhoeffer, P.R. Dunbar, M.A. Nowak, S. Monard, J.P. Segal, Y. Cao, S.L. Rowland-Jones, V. Cerundolo, A. Hurley, M. Markowitz, D.D. Ho, D.F. Nixon, A.J. McMichael, Quantitation of HIV-1-specific cytotoxic T lymphocytes and plasma load of viral RNA, Science 279 (1998) 2103–2106.

[10] C. Hess, M. Altfeld, S.Y. Thomas, M.M. Addo, E.S. Rosenberg, T.M. Allen, R. Draenert, R.L. Eldrige, J.V. Luzen, H.J. Stellbrink, B.D. Walker, A.D. Luster, HIV-1 specific CD8+T cells with an effector phenotype and control of viral replication, Lancet 363 (2004) 863–866.

[11] E.S. Rosenberg, J.M. Billingsley, A.M. Caliendo, S.L. Boswell, P.E. Sax, S.A. Kalams, B.D. Walker, Vigorous HIV-1-specific CD4+T cell responses associated with control of viremia, Science 278 (1997) 1447–1450.

[12] D.E. Smith, B.D. Walker, D.A. Cooper, E.S. Rosenberg, J.M. Kaldor, Is antiretroviral treatment of primary HIV infection clinically justified on the basis of current evidence? AIDS 18 (2004) 709–718.

[13] F.M. Hecht, L. Wang, A. Collier, S. Little, M. Markowitz, J. Margolick, J.M. Kilby, E. Daar, B. Conway, S. Holtefor the AIEDRP Network, A multicenter observational study of the potential benefits of initiating combination antiretroviral therapy during acute HIV infection, J. Infect. Dis. 194 (2006) 725–733.

[14] C.L. Tremblay, J.L. Hicks, L. Sutton, F. Giguel, T. Flynn, M. Johnston, P.E. Sax, B.D. Walker, M.S. Hirsh, E.S. Rosenberg, R.T. D'Aquila, Antiretroviral resistance associated with supervised treatment interruptions in treated acute HIV infection, AIDS 17 (2003) 1086–1089.

[15] D.E. Kaufmann, M. Lichterfeld, M. Altfeld, M.M. Addo, M.N. Johnston, P.K. Lee, B.S. Wagner, E.T. Kalife, D. Strick, E.S. Rosenberg, B.D. Walker, Limited durability of viral control following treated acute HIV infection, PLoS Med. 1 (2004) e36.

[16] T.M. Allen, D.H. O'Connor, P. Jing, J.L. Dzuris, B.R. Mothe, T.U. Vogel, E. Dunphy, M.E. Lieble, C. Emerson, N. Wilson, K.J. Kunstman, X. Wang, D.B. Allison, A.L. Hughes, R.C. Desrosiers, J.D. Altman, S.M. Wolinsky, A. Sette, D.I. Watkins, Tat-specific cytotoxic T lymphocytes select for SIV escape variants during resolution of primary viraemia, Nature 407 (2000) 386–390.

[17] D.T. Evans, D.H. O'Connor, P. Jing, J.L. Dzuris, J. Sydney, J. da Silva, T.M. Allen, H. Horton, J.E. Venham, R.A. Rudersdorf, T. Vogel, C.D. Pauze, R.E. Bontrop, R. DeMars, A. Sette, A.L. Hughes, D.I. Watkins, Virus-specific cytotoxic T lymphocyte responses select for amino-acid variation in simian immunodeficiency virus Env and Nef, Nat. Med. 5 (1999) 1270–1276.

[18] D.H. Barouch, J. Kunstman, M.J. Kuroda, J.E. Schmits, S. Santra, F.W. Peyerl, G.R. Gorgone, D.C. Montefiori, M.G. Lewis, S.M. Wolinsky, N.L. Letvin, Viral escape from dominant simian immunodeficiency virus epitope-specific cytotoxic T lymphocytes in DNA-vaccinated rhesus monkeys, J. Virol. 77 (2003) 7367–7375.

[19] C.B. Moore, M. John, I.R. James, F.T. Christriansen, C.S. Witt, S.A. Mallal, Evidence of HIV-1 adaptation to HLA-restricted immune responses at a population level, Science 296 (2002) 1439–1443.

[20] P.J. Goulder, C. Brander, Y. Tang, C.A. Tremblay, R.A. Colbert, M.M. Addo, E.S. Rosenberg, T. Nguyen, R. Allen, A. Trocha, M. Altfeld, S. He, M. Bunce, R. Funkhouser, S.I. Pelton, S.K. Burchett, K. McIntosh, B.T. Korber, B.D. Walker, Evolution and transmission of stable CTL escape mutations in HIV infection, Nature 412 (2001) 334–338.

[21] T. Furutsuki, N. Hosoya, A. Kawana-Tachikawa, M. Tomizawa, T. Odawara, M. Goto, Y. Kitamura, T. Nakamura, A.D. Kelleher, D.A. Cooper, A. Iwamoto, Frequent transmission of cytotoxic-T-lymphocyte escape mutants of human immunodeficiency virus type 1 in the highly HLA-A-24-positive Japanese population, J. Virol. 78 (2004) 8437–8445.

[22] Y. Ikeda-Moore, H. Tomiyama, K. Miwa, S. Oka, A. Iwamoto, Y. Kaneko, M. Takiguchi, Identification and characterization of multiple HLA-A24-restricted HIV-1 CTL epitopes: Strong epitopes are derived from V regions of HIV-1, J. Immunol. 159 (1997) 6242–6252.

[23] M. Fujiwara, J. Tanuma, H. Koizumi, Y. Kawashima, K. Honda, S. Matsuoka-Aizawa, S. Dohki, S. Oka, M. Takiguchi, Different abilities of escape mutant-specific cytotoxic T cells to suppress replication of escape mutant and wild-type human immunodeficiency virus type 1 in new hosts, J. Virol. 82 (2008) 138–147.

[24] V.A. Johnson, F. Brun-Vezinet, B. Clotet, D.R. Kuritzkes, D. Pillay, J.M. Schapiro, D.D. Richman, Update of the drug resistance mutations in HIV-1: Fall 2006, Top. HIV Med. 14 (2006) 125–130.

[25] J.D. Altman, P.A.H. Moss, P.J.R. Goulder, D.H. Barouch, M.G. McHeyzer-Williams, J.I. Bell, A.J. McMichael, M.M. Davis,

Phenotypic analysis of antigen-specific T lymphocytes, Science 274 (1996) 94–96.
[26] M. Carrington, S.J. O'Brien, The influence of HLA genotype on AIDS, Annu. Rev. Med. 54 (2003) 535–551.
[27] H. Tomiyama, H. Akari, A. Adachi, M. Takiguchi, Different effects of Nef-mediated HLA class I down-regulation on human immunodeficiency virus type 1-specific CD8+T-cell cytolytic activity and cytokine production, J. Virol. 76 (2002) 7535–7543.
[28] H. Tomiyama, M. Fujiwara, S. Oka, M. Takiguchi, Epitope-dependent effect of Nef-mediated HLA class I down-regulation on ability of HIV-1-specific CTLs to suppress HIV-1 replication, J. Immunol. 174 (2005) 36–40.
[29] Y. Yokomaku, H. Miura, H. Tomiyama, A. Kawana-Tachikawa, M. Takiguchi, A. Kojima, Y. Nagai, A. Iwamoto, Z. Matsuda, K. Ariyoshi, Impaired processing and presentation of cytotoxic-T-lymphocyte (CTL) epitopes are major escape mechanisms from CTL immune pressure in human immunodeficiency virus type 1 infection, J. Virol. 78 (2004) 1324–1332.

Journal of
Medicinal Chemistry

Letter

Design of a Novel HIV-1 Fusion Inhibitor That Displays a Minimal Interface for Binding Affinity

Shinya Oishi, Saori Ito, Hiroki Nishikawa, Kentaro Watanabe, Michinori Tanaka, Hiroaki Ohno, Kazuki Izumi, Yasuko Sakagami, Eiichi Kodama, Masao Matsuoka, and Nobutaka Fujii

J. Med. Chem., **2008**, 51 (3), 388-391• DOI: 10.1021/jm701109d • Publication Date (Web): 16 January 2008

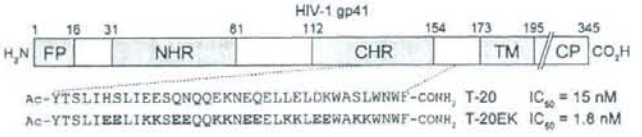

More About This Article

Additional resources and features associated with this article are available within the HTML version:

- Supporting Information
- Access to high resolution figures
- Links to articles and content related to this article
- Copyright permission to reproduce figures and/or text from this article

View the Full Text HTML

Journal of Medicinal Chemistry is published by the American Chemical Society.
1155 Sixteenth Street N.W., Washington, DC 20036

Design of a Novel HIV-1 Fusion Inhibitor That Displays a Minimal Interface for Binding Affinity

Shinya Oishi,*,† Saori Ito,† Hiroki Nishikawa,† Kentaro Watanabe,† Michinori Tanaka,† Hiroaki Ohno,† Kazuki Izumi,‡ Yasuko Sakagami,‡ Eiichi Kodama,‡ Masao Matsuoka,‡ and Nobutaka Fujii*,†

Graduate School of Pharmaceutical Sciences, Kyoto University, Sakyo-ku, Kyoto 606-8501, Japan, and Laboratory of Virus Immunology, Institute for Virus Research, Kyoto University, Sakyo-ku, Kyoto 606-8507, Japan

Received September 6, 2007

Abstract: Reported herein are the design, biological activities, and biophysical properties of a novel HIV-1 membrane fusion inhibitor. α-Helix-inducible X-EE-XX-KK motifs were applied to design an enfuvirtide analogue **2** that exhibited highly potent anti-HIV activity against wild-type HIV-1, enfuvirtide-resistant HIV-1 strains, and an HIV-2 strain in vitro. Indispensable residues for bioactivity of enfuvirtide, including the residues interacting with the N-terminal heptad repeat and the C-terminal hydrophobic residues, were identified.

The viral entry process of human immunodeficiency virus type 1 (HIV-1[a]) into target cells is mediated by envelope glycoprotein gp41. Formation of a fusogenic six-helical bundle structure consisting of a gp41 N-terminal heptad repeat (NHR) and C-terminal heptad repeat (CHR) promotes the fusion of viral and cellular membranes (Figure 1a).[1] Enfuvirtide **1** (T-20, DP178) is an approved anti-HIV peptide derived from the gp41 CHR.[2,3] This first drug that inhibits HIV-1 entry into the cell is utilized as an alternative anti-HIV agent for patients with drug resistance to reverse transcriptase and/or protease inhibitors. It is believed that peptide **1** interacts with the NHR of gp41 prehairpin structure[4] and associates with the cell or viral membrane through a C-terminal tryptophan-rich region,[5–7] but the exact action mechanism of **1** has not been clarified.[8,9]

Stabilization of bioactive conformations of peptides is a promising approach to enhance their biological potency and to understand the bioactive conformation. Several approaches to stabilize the α-helix structure of gp41 CHR have been reported including macrocyclization by covalent bond formation[10] or salt-bridge formation[11–13] between two adjacent residues and/or introduction of α-helix-inducible peptide sequences.[11] The analogue of another CHR peptide C34, in which the residues on the outer surface of the six-helical bundle were comprehensively replaced with glutamates (Glu) or lysines (Lys), retained highly potent anti-HIV activity.[12] This indicates that the substituted residues are not associated with an NHR coiled-coil as suggested by the crystal structure of the N36-C34 complex.[14] Our expectation was that the following three functional surfaces of **1** could be characterized by extending this molecular design (Figure 1b): (1) minimal interface residues for affinity with NHR; (2) solvent-accessible sites to be utilized for α-helix inducible salt bridges; (3) another functional region outside the α-helix structure. Accordingly, efforts herein were undertaken to design novel amphiphilic enfuvirtide derivatives bearing α-helix-inducible motifs.

A schematic wheel of the potential α-helix structure of peptide **1** is depicted in Figure 1c. To introduce salt bridges between i and $i + 4$ residues on the basis of the previous C34 modification,[12] Glu and Lys were arranged at b/c and f/g positions, respectively, so that four consecutive X-EE-XX-KK motifs appeared in the designed peptide **2** (designated T-20EK, Figure 2). All peptides were prepared by standard Fmoc-based peptide synthesis protocol. After final deprotection and cleavage from the resins using a TFA/thioanisole/*m*-cresol/ethanedithiol/H_2O (80:5:5:5:5) cocktail, the crude peptides were purified by reverse-phase HPLC to yield the expected peptides, which were characterized by mass spectrometry. Anti-HIV activity of the peptides against laboratory HIV-1 NL4-3 strain (wild-type) was evaluated by MAGI assay (Table 1). Peptide **2** exhibited 8-fold greater anti-HIV activity compared with the parent peptide **1** [peptide **1**, $EC_{50} = 15 \pm 3.9$ nM; peptide **2**, $EC_{50} = 1.8 \pm 0.4$ nM].[15] The circular dichroism (CD) spectrum of **2** in phosphate buffered saline (pH 7.4) had negative minima at 208 and 222 nm, indicating the presence of an α-helical conformation, while that of **1** suggested a random-coil conformation (Figure 3a). The significant increase in anti-HIV activity of **2** could be rationalized by the preordered stable α-helical structure upstream of L158.[16]

Systematic substitutions of the amino acids at the b, c, f, and g positions with Glu or Lys were extended (Figure 2). Peptide **3**, in which L130 and N160 were substituted with Lys and Glu, respectively, showed anti-HIV activity similar to that of peptide **2** (peptide **3**, $EC_{50} = 2.8 \pm 0.6$ nM). This is consistent with the fact that potent T-1249 also contains these two substitutions.[17] Further replacement toward the N-terminal f position (S129) was again permissive of the high anti-HIV activity (peptide **4**, $EC_{50} = 2.5 \pm 0.6$ nM). On the other hand, replacement of W161 with Glu resulted in a significant decrease of anti-HIV activity as observed in peptides **5** and **6** ($EC_{50} = 185$ and 111 nM, respectively), indicating that W161 may be located outside the amphiphilic α-helical region. This result correlates with the reduced entry ability of W161F mutant virus.[18] Alanine substitution of W161 also supports the relevance of this residue in virus infectivity and in the inhibitory activity of **1**. Although peptide **7**, carrying a W155A substitution, expressed anti-HIV activity similar to that of peptide **2** (peptide **7**, $EC_{50} = 5.8 \pm 1.0$ nM), W159A, W161A, and F162A substitutions showed reduced bioactivity (peptides **8**, **9**, and **10**, $EC_{50} = 49$, 24, and 27 nM, respectively). The observed similar CD spectra among peptides **2** and **7–10** demonstrated that alanine substitution had no effect on the stabilized secondary structure of the α-helix (Figure 3b). That is, the hydrophobic indole and phenyl groups of these peptides may contribute to their direct interaction with virus components such as gp41 NHR or the virus membrane.[19]

The comparative binding affinity of peptides **1** and **2** with the gp41 NHR sequence was investigated by pull-down assay using synthetic His-tagged CHR peptides and recombinant MBP-fused NHR protein (Figure 4a). Peptide **2** showed higher affinity with NHR compared with **1**. In contrast, only weak binding was observed in the same experiment using all-D-T-20EK D-**2**, which consists of all D-amino acids, indicating that

* To whom correspondence should be addressed. Phone: +81-75-753-4551. Fax: +81-75-753-4570. E-mail: for S.O., soishi@pharm.kyoto-u.ac.jp; for N.F., nfujii@pharm.kyoto-u.ac.jp.

† Graduate School of Pharmaceutical Sciences.

‡ Institute for Virus Research.

[a] Abbreviations: HIV-1, human immunodeficiency virus type 1; NHR, N-terminal heptad repeat; CHR, C-terminal heptad repeat.

10.1021/jm701109d CCC: $40.75
Published on Web 01/16/2008

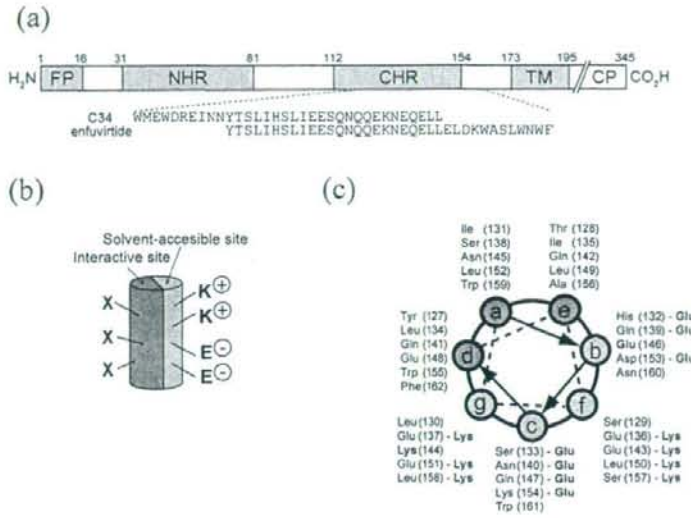

Figure 1. Design of enfuvirtide analogues: (a) schematic representation of HIV-1 gp41 (FP, fusion peptide; NHR, N-terminal heptad repeat; CHR, C-terminal heptad repeat; TM, transmembrane domain); (b) estimated preordered α-helix structure of CHR peptide by potential salt-bridge formation; (c) helical-wheel representation of peptides **1** and **2**. For peptide **2**, Glu residues are in b and e positions and Lys residues in f and g positions. Residues are numbered starting at the first amino acid of the NL4-3 gp41.

```
Ac-YTSLIHSLIEESQNQQEKNEQELLELDKWASLWNWF-CONH2   1 (enfuvirtide)
Ac------EE--KK-EE--K---E--KK-EE--KK-----CONH2   2
Ac----K-EE--KK-EE--K---E--KK-EE--KK-E---CONH2   3
Ac---KK-EE--KK-EE--K---E--KK-EE--KK-E---CONH2   4
Ac----K-EE--KK-EE--K---E--KK-EE--KK-EE--CONH2   5
Ac---KK-EE--KK-EE--K---E--KK-EE--KK-EE--CONH2   6
Ac------EE--KK-EE--K---E--KK-EEA-KK-----CONH2   7
Ac------EE--KK-EE--K---E--KK-EE--KKA----CONH2   8
Ac------EE--KK-EE--K---E--KK-EE--KK--A--CONH2   9
Ac------EE--KK-EE--K---E--KK-EE--KK---A-CONH2   10
   Ac-LDAN-TK-L--A-I-----MY--QK-NQ-DIFS----CONH2   11
Ac-WQEWEQK-TA-L-QA-I------Y--QK--------E---CONH2   T-1249
```

Figure 2. Peptide sequences of enfuvirtide, enfuvirtide analogues, and T-1249.

Table 1. Anti-HIV Activity of Synthetic Enfuvirtide Analogues

peptide	EC_{50} (nM)[a]	peptide	EC_{50} (nM)[a]
1 (enfuvirtide)	15 ± 3.9	**7**	5.8 ± 1.0
2[b]	1.8 ± 0.4	**8**	49 ± 8.6
3	2.8 ± 0.6	**9**	24 ± 3.8
4	2.5 ± 0.6	**10**	27 ± 6.8
5	185 ± 17	C34	4.5 ± 0.5
6	111 ± 25		

[a] EC_{50} was determined as the concentration that blocked HIV-1 replication by 50% in MAGI assay. [b] The enantiomer of peptide **2** (D-**2**) did not show anti-HIV activity at 10 μM.

the binding between **2** and NHR is specific. In addition, peptide **2** inhibited the interaction between **1** and NHR in lower concentration in the inhibition experiment (Figure 4b).[20]

We next evaluated the anti-HIV activity of peptide **2** against enfuvirtide-resistant variants HIV-1_{V38A} and HIV-1_{N43D}, which were mainly isolated from patients resistant to enfuvirtide (Table 2).[21] Because of the deficient replication of these variants,[22] an additional D36G mutation was experimentally added to these variants and to the wild-type virus. The D36G mutation is not involved in enfuvirtide resistance, but it did improve the sensitivity against **1** [EC_{50}(HIV-1_{D36G}) = 2.3 nM] compared with wild-type HIV-1. As reported previously,[21] V38A and N43D mutations significantly reduced the potency of **1** [EC_{50}(HIV-1_{V38A}) = 22 nM; EC_{50}(HIV-1_{N43D}) = 46 nM]. On the other hand, peptide **2** retained similar anti-HIV activity against N43D and slightly less potent activity toward V38A variants [EC_{50}(HIV-1_{V38A}) = 3.3 nM; EC_{50}(HIV-1_{N43D}) = 1.7 nM]. It is of interest that the anti-HIV activity was restored by induction of a bioactive α-helix structure using X-EE-XX-KK motifs on a CHR peptide. This implies that the stable α-helical structure of **2** can overcome the reduced affinity derived from the mismatched interaction between mutated NHR sequences and peptide **1**.

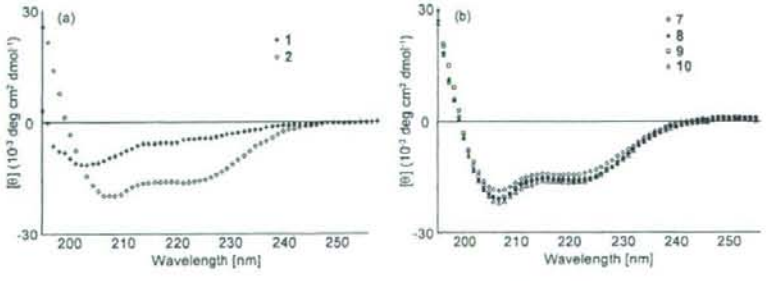

Figure 3. Circular dichroism spectra of (a) peptides **1** and **2** and (b) Ala-substituted peptides **7**–**10**.

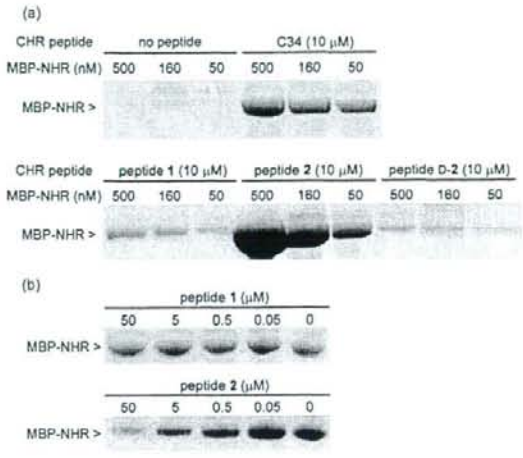

Figure 4. Interaction of His-tagged CHR peptides with MBP-NHR protein by pull-down assay and SDS−PAGE: (a) NHR protein binding with several His-tagged CHR peptides; (b) inhibition of interaction between His-tagged enfuvirtide and NHR protein by nontagged peptides **1** and **2**.

Table 2. Anti-HIV Activity of Peptides **1** and **2** against Enfuvirtide-Resistant Variant and HIV-2 Strains

	EC_{50} (nM)[a]	
strains	peptide **1**	peptide **2**
HIV-1		
NL4–3	15 ± 3.9	1.8 ± 0.4
D36G	2.3 ± 0.5	0.9 ± 0.2
D36G V38A	22 ± 7.6	3.3 ± 1.0
D36G N43D	46 ± 9.6	1.7 ± 0.3
HIV-2		
EHO[b]	37 ± 10	1.5 ± 0.5

[a] EC_{50} was determined as the concentration that blocked HIV-1 replication by 50% in MAGI assay. [b] The antiviral activity (EC_{50}) of peptide **11** against EHO strain was 2.1 ± 0.7 nM.

Interestingly, peptide **2** showed potent antiviral activity even against an HIV-2 EHO strain [EC_{50} = 1.5 nM], which is as potent as peptide **11** having a congenerous sequence derived from the EHO strain [EC_{50} = 2.1 nM].[23] This is in contrast to the previous report on the reduced activity of **1** against the EHO strain [EC_{50} = 37 nM].[24] The potent bioactivity of **2** can be rationalized by the minimal difference of the interface residues between HIV-1 and -2 and the stabilized α-helix structure. Among 19 different residues between the sequences of NL4-3 and EHO strains, 13 residues are located at the solvent accessible sites (b, c, f, and g positions). Although the other six residues are possibly involved in the direct interaction, the potential reduced interactions derived from the mismatch could be recovered by introduction of X-EE-XX-KK motifs.

In conclusion, remodeling of **1** to yield the preordered α-helical structure of **2** led to improved affinity with NHR and increased antiviral activity even against enfuvirtide-resistant HIV-1 and HIV-2 strains. This approach also helped to clarify the potential minimal interface of **1** with viral gp41. Peptide **2** could be a useful chemical tool to understand the membrane fusion process of HIV-1 and the detailed action mechanism of enfuvirtide.

Acknowledgment. This work was supported by a Grant-in-Aid for Scientific Research from the Ministry of Education, Culture, Sports, Science, and Technology of Japan, Health and Labour Sciences Research Grants (Research on HIV/AIDS), the 21st Century COE Program's "Knowledge Information Infrastructure for Genome Science", and the Japan Science and Technology Agency. H.N. is grateful for the JSPS Research Fellowships for Young Scientists. Appreciation is expressed to Dr. Masaru Hoshino (Kyoto University) for helpful discussions and to Mr. Maxwell Reback (Kyoto University) for reading the manuscript.

Supporting Information Available: Experimental details for peptide preparation, CD spectra measurements, and bioassays and MS and HPLC data. This material is available free of charge via the Internet at http://pubs.acs.org.

References

(1) Lu, M.; Blacklow, S. C.; Kim, P. S. A trimeric structural domain of the HIV-1 transmembrane glycoprotein. *Nat. Struct. Biol.* **1995**, *2*, 1075–1082.
(2) Wild, C. T.; Shugars, D. C.; Greenwell, T. K.; McDanal, C. B.; Matthews, T. J. Peptides corresponding to a predictive alpha-helical domain of human immunodeficiency virus type 1 gp41 are potent inhibitors of virus infection. *Proc. Natl. Acad. Sci. U.S.A.* **1994**, *91*, 9770–9774.
(3) Matthews, T.; Salgo, M.; Greenberg, M.; Chung, J.; DeMasi, R.; Bolognesi, D. Enfuvirtide: the first therapy to inhibit the entry of HIV-1 into host CD4 lymphocytes. *Nat. Rev. Drug. Discovery* **2004**, *3*, 215–225.
(4) Lawless, M. K.; Barney, S.; Guthrie, K. I.; Bucy, T. B.; Petteway, S. R., Jr.; Merutka, G. HIV-1 membrane fusion mechanism: structural studies of the interactions between biologically-active peptides from gp41. *Biochemistry* **1996**, *35*, 13697–13708.
(5) Kliger, Y.; Gallo, S. A.; Peisajovich, S. G.; Munoz-Barroso, I.; Avkin, S.; Blumenthal, R.; Shai, Y. Mode of action of an antiviral peptide from HIV-1. Inhibition at a post-lipid mixing stage. *J. Biol. Chem.* **2001**, *276*, 1391–1397.
(6) Cardoso, R. M.; Zwick, M. B.; Stanfield, R. L.; Kunert, R.; Binley, J. M.; Katinger, H.; Burton, D. R.; Wilson, I. A. Broadly neutralizing anti-HIV antibody 4E10 recognizes a helical conformation of a highly conserved fusion-associated motif in gp41. *Immunity* **2005**, *22*, 163–173.
(7) Wexler-Cohen, Y.; Johnson, B. T.; Puri, A.; Blumenthal, R.; Shai, Y. Structurally altered peptides reveal an important role for N-terminal heptad repeat binding and stability in the inhibitory action of HIV-1 peptide DP178. *J. Biol. Chem.* **2006**, *281*, 9005–9010.
(8) Liu, S.; Lu, H.; Niu, J.; Xu, Y.; Wu, S.; Jiang, S. Different from the HIV fusion inhibitor C34, the anti-HIV drug Fuzeon (T-20) inhibits HIV-1 entry by targeting multiple sites in gp41 and gp120. *J. Biol. Chem.* **2005**, *280*, 11259–11273.
(9) Liu, S.; Jing, W.; Cheung, B.; Lu, H.; Sun, J.; Yan, X.; Niu, J.; Farmar, J.; Wu, S.; Jiang, S. HIV gp41 C-terminal heptad repeat contains multifunctional domains. Relation to mechanisms of action of anti-HIV peptides. *J. Biol. Chem.* **2007**, *282*, 9612–9620.
(10) Judice, J. K.; Tom, J. Y.; Huang, W.; Wrin, T.; Vennari, J.; Petropoulos, C. J.; McDowell, R. S. Inhibition of HIV type 1 infectivity by constrained α-helical peptides: implications for the viral fusion mechanism. *Proc. Natl. Acad. Sci. U.S.A.* **1997**, *94*, 13426–13430.
(11) Joyce, J. G.; Hurni, W. M.; Bogusky, M. J.; Garsky, V. M.; Liang, X.; Citron, M. P.; Danzeisen, R. C.; Miller, M. D.; Shiver, J. W.; Keller, P. M. Enhancement of α-helicity in the HIV-1 inhibitory peptide DP178 leads to an increased affinity for human monoclonal antibody 2F5 but does not elicit neutralizing responses in vitro. *J. Biol. Chem.* **2002**, *277*, 45811–45820.
(12) Otaka, A.; Nakamura, M.; Nameki, D.; Kodama, E.; Uchiyama, S.; Nakamura, S.; Nakano, H.; Tamamura, H.; Kobayashi, Y.; Matsuoka, M.; Fujii, N. Remodeling of gp41-C34 peptide leads to highly effective inhibitors of the fusion of HIV-1 with target cells. *Angew. Chem., Int. Ed.* **2002**, *41*, 2937–2940.
(13) Dwyer, J. J.; Wilson, K. L.; Davison, D. K.; Freel, S. A.; Seedorff, J. E.; Wring, S. A.; Tvermoes, N. A.; Matthews, T. J.; Greenberg, M. L.; Delmedico, M. K. Design of helical, oligomeric HIV-1 fusion inhibitor peptides with potent activity against enfuvirtide-resistant virus. *Proc. Natl. Acad. Sci. U.S.A.* **2007**, *104*, 12772–12777.
(14) Chan, D. C.; Fass, D.; Berger, J. M.; Kim, P. S. Core structure of gp41 from the HIV envelope glycoprotein. *Cell* **1997**, *89*, 263–273.
(15) Cytotoxicity of peptide **2** was not observed even at 10 μM.
(16) Additional effects on increasing the anti-HIV activity such as formation of intra- and intermolecular salt bridges are also possible.
(17) Eron, J. J.; Gulick, R. M.; Bartlett, J. A.; Merigan, T.; Arduino, R.; Kilby, J. M.; Yangco, B.; Diers, A.; Drobnes, C.; DeMasi, R.;

Greenberg, M.; Melby, T.; Raskino, C.; Rusnak, P.; Zhang, Y.; Spence, R.; Miralles, G. D. Short-term safety and antiretroviral activity of T-1249, a second-generation fusion inhibitor of HIV. *J. Infect. Dis.* **2004**, *189*, 1075–1083.

(18) Salzwedel, K.; West, J. T.; Hunter, E. A conserved tryptophan-rich motif in the membrane-proximal region of the human immunodeficiency virus type 1 gp41 ectodomain is important for Env-mediated fusion and virus infectivity. *J. Virol.* **1999**, *73*, 2469–2480.

(19) Wexler-Cohen, Y.; Johnson, B. T.; Puri, A.; Blumenthal, R.; Shai, Y. Structurally altered peptides reveal an important role for N-terminal heptad repeat binding and stability in the inhibitory action of HIV-1 peptide DP178. *J. Biol. Chem.* **2006**, *281*, 9005–9010.

(20) Since a large excess of CHR peptides to NHR protein was utilized for the pull-down assay, the inhibitory concentration in this experiment was less than that observed in the MAGI assay. It is conceivable that the anti-HIV activity in the MAGI assay might be observed with less fully occupied one or two CHR peptides bound per NHR trimer.

(21) Cabrera, C.; Marfil, S.; Garcia, E.; Martinez-Picado, J.; Bonjoch, A.; Bofill, M.; Moreno, S.; Ribera, E.; Domingo, P.; Clotet, B.; Ruiz, L. Genetic evolution of gp41 reveals a highly exclusive relationship between codons 36, 38 and 43 in gp41 under long-term enfuvirtide-containing salvage regimen. *AIDS* **2006**, *20*, 2075–2080.

(22) Mink, M.; Mosier, S. M.; Janumpalli, S.; Davison, D.; Jin, L.; Melby, T.; Sista, P.; Erickson, J.; Lambert, D.; Stanfield-Oakley, S. A.; Salgo, M.; Cammack, N.; Matthews, T.; Greenberg, M. L. Impact of human immunodeficiency virus type 1 gp41 amino acid substitutions selected during enfuvirtide treatment on gp41 binding and antiviral potency of enfuvirtide in vitro. *J. Virol.* **2005**, *79*, 12447–12454.

(23) Gustchina, E.; Hummer, G.; Bewley, C. A.; Clore, G. M. Differential inhibition of HIV-1 and SIV envelope-mediated cell fusion by C34 peptides derived from the C-terminal heptad repeat of gp41 from diverse strains of HIV-1, HIV-2, and SIV. *J. Med. Chem.* **2005**, *48*, 3036–3044.

(24) Witvrouw, M.; Pannecouque, C.; Switzer, W. M.; Folks, T. M.; De Clercq, E.; Heneine, W. Susceptibility of HIV-2, SIV and SHIV to various anti-HIV-1 compounds: implications for treatment and post-texposure prophylaxis. *Antiviral Ther.* **2004**, *9*, 57–65.

JM701109D

JOURNAL OF VIROLOGY, Jan. 2008, p. 764–774 Vol. 82, No. 2
0022-538X/08/$08.00+0 doi:10.1128/JVI.01534-07

Broad Antiretroviral Activity and Resistance Profile of the Novel Human Immunodeficiency Virus Integrase Inhibitor Elvitegravir (JTK-303/GS-9137)▽†

Kazuya Shimura,[1] Eiichi Kodama,[1]* Yasuko Sakagami,[1] Yuji Matsuzaki,[2] Wataru Watanabe,[2]‡ Kazunobu Yamataka,[2] Yasuo Watanabe,[2] Yoshitsugu Ohata,[2] Satoki Doi,[3] Motohide Sato,[2] Mitsuki Kano,[2] Satoru Ikeda,[2] and Masao Matsuoka[1]

Laboratory of Virus Immunology, Institute for Virus Research, Kyoto University, 53 Kawaramachi, Shogoin, Sakyo-ku, Kyoto 606-8507, Japan[1]; Japan Tobacco Inc., Central Pharmaceutical Research Institute, 1-1 Murasaki-cho, Takatsuki, Osaka 569-1125, Japan[2]; and Japan Tobacco Inc., Central Pharmaceutical Research Institute, Pharmaceutical Frontier Research Laboratories, 1-13-2 Fukuura, Kanazawa-Ku, Yokohama, Kanagawa 236-0004, Japan[3]

Received 13 July 2007/Accepted 22 October 2007

Integrase (IN), an essential enzyme of human immunodeficiency virus (HIV), is an attractive antiretroviral drug target. The antiviral activity and resistance profile in vitro of a novel IN inhibitor, elvitegravir (EVG) (also known as JTK-303/GS-9137), currently being developed for the treatment of HIV-1 infection are described. EVG blocked the integration of HIV-1 cDNA through the inhibition of DNA strand transfer. EVG inhibited the replication of HIV-1, including various subtypes and multiple-drug-resistant clinical isolates, and HIV-2 strains with a 50% effective concentration in the subnanomolar to nanomolar range. EVG-resistant variants were selected in two independent inductions, and a total of 8 amino acid substitutions in the catalytic core domain of IN were observed. Among the observed IN mutations, T66I and E92Q substitutions mainly contributed to EVG resistance. These two primary resistance mutations are located in the active site, and other secondary mutations identified are proximal to these primary mutations. The EVG-selected IN mutations, some of which represent novel IN inhibitor resistance mutations, conferred reduced susceptibility to other IN inhibitors, suggesting that a common mechanism is involved in resistance and potential cross-resistance. The replication capacity of EVG-resistant variants was significantly reduced relative to both wild-type virus and other IN inhibitor-resistant variants selected by L-870,810. EVG and L-870,810 both inhibited the replication of murine leukemia virus and simian immunodeficiency virus, suggesting that IN inhibitors bind to a conformationally conserved region of various retroviral IN enzymes and are an ideal drug for a range of retroviral infections.

Three unique and essential HIV enzymes, protease (PR), reverse transcriptase with RNase H (RT), and integrase (IN), appear to be ideal targets for the development of inhibitors of human immunodeficiency virus (HIV) replication. Anti-HIV drugs targeting PR (PR inhibitors [PIs]) and RT (nucleoside/nucleotide RT inhibitors [NRTIs] and nonnucleoside RT inhibitors [NNRTIs]) have been approved for use in the treatment of HIV infection. Combinations of these drugs used in highly active antiretroviral therapy can effectively suppress HIV replication in vivo to undetectable levels and have led to significant declines in HIV-associated mortality (28, 40). However, the emergence of drug-resistant HIV variants can attenuate the efficacy of antiretroviral treatment. Some primary infections also result from the transmission of HIV strains that possess drug-resistant genotypes and phenotypes (9). To suppress these drug-resistant variants, new anti-HIV drugs that block new targets are urgently needed.

IN, a 32-kDa protein resulting from the proteolytic cleavage of the *gag-pol* precursor, plays an essential role in the integration of proviral DNA into the host genome. As LaFemina et al. previously reported that there is no human homologue of HIV IN (31), it is an attractive target for the development of new antiretroviral therapeutic agents without adverse effects. IN consists of three domains: an N-terminal zinc finger domain and a C-terminal DNA-binding domain flank a central catalytic core domain (CCD) that plays a critical role in its enzymatic activity (13, 14). Following reverse transcription, IN exerts at least two functions: the cleavage of two conserved nucleotides from the 3′ ends of both strands of the viral cDNA (3′ processing) (1) and, subsequently, the ligation of the viral cDNA into the host genome (strand transfer) (14). Gap filling of the interfaces between the viral and host genomic DNA is then completed using the host DNA repair machinery via a mechanism that is not yet fully understood. The completion of integration results in a fully functional provirus, which can then be used to initiate viral DNA transcription.

Several compounds that inhibit IN activity have been described, including diketo acid (DKA) derivatives such as L-731,988 (24) and S-1360 (16), both of which have potent

* Corresponding author. Mailing address: Laboratory of Virus Immunology, Institute for Virus Research, Kyoto University, 53 Kawaramachi, Shogoin, Sakyo-ku, Kyoto 606-8507, Japan. Phone and fax: 81-75-751-3986. E-mail: ekodama@virus.kyoto-u.ac.jp.

† Supplemental material for this article may be found at http://jvi.asm.org/.

‡ Present address: Kyushu University of Health and Welfare, 1714-1 Yoshinomachi, Nobeoka, Miyazaki 882-8508, Japan.

▽ Published ahead of print on 31 October 2007.

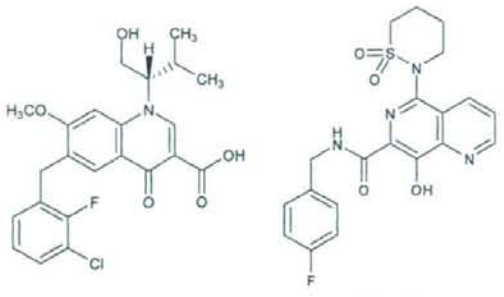

FIG. 1. Structure of EVG and L-870,810. A dihydroquinoline carboxylic acid derivative, EVG, and a naphthyridine carboxamide derivative, L-870,810 (a representative IN inhibitor), are shown.

antiviral activity. Crystal structure analysis has indicated that 1-(5-chloroindol-3-yl)-3-hydroxy-3-(2*H*-tetrazol-5-yl)-propenone, an S-1360 derivative, binds to the CCD, the putative active site of IN (19). In vitro resistance selection experiments with several IN inhibitors demonstrated that mutations in the CCD of IN play a significant role in the generation of IN inhibitor-resistant viral variants. In vitro selection of HIV-1 in the presence of the DKA IN inhibitors L-731,988 and S-1360 resulted in the emergence of viral variants carrying IN mutations associated with resistance. These mutations, including T66I, S153Y, and M154I, are located in close proximity to the catalytic triad residues (D64, D116, and E152) in the CCD of IN (16, 24). In contrast, L-870,810 (Fig. 1), which has previously demonstrated potent antiviral activity in HIV-1-infected patients in a monotherapy study (33), induced unique IN mutations, including V72I, F121Y, T125K, and V151I, when HIV was selected with the compound in vitro (23). These mutations are also located in the active site of IN, suggesting that a common mechanism may be involved in the acquisition of resistance to IN inhibitors.

Although no IN inhibitors are currently approved for clinical use (41), two IN inhibitors, elvitegravir (EVG) (formerly known as JTK-303/GS-9137, being codeveloped by Gilead Sciences and Japan Tobacco) (Fig. 1) (43, 56) and raltegravir (MK-0518, developed by Merck) (22), are currently being investigated in clinical studies of HIV-1-infected patients. In a phase II study, antiretroviral treatment-experienced patients using 125 mg EVG (boosted with ritonavir) along with an active optimized background regimen showed >2-$\log_{10}$ declines in their viral loads that were durable through week 24 (56).

Here, we describe the antiviral activity, mechanism of action, and resistance profile of EVG in vitro. EVG exerted potent anti-HIV activity against not only wild-type strains but also drug-resistant clinical isolates. Interestingly, EVG also showed antiviral activity against murine leukemia virus (MLV) and simian immunodeficiency virus (SIV). These results imply that IN inhibitors are ideal agents for the treatment of a range of retroviral infections. During the selection of EVG-resistant viral variants, novel IN mutations emerged. Combinations of these mutations conferred resistance to EVG and reduced susceptibility to other IN inhibitors, suggesting that there is a common mechanism underlying the resistance to IN inhibitors. One such mechanism may be conformational changes induced by multiple mutations located in the active site of IN.

MATERIALS AND METHODS

Antiviral agents. Zidovudine (AZT) and dextran sulfate (DS5000) (average molecular weight, 5,000) were purchased from Sigma (St. Louis, MO). Efavirenz (EFV) (NNRTI) and nelfinavir (NFV) (PI) were used for the control inhibitor. EVG (43), L-731,988 (42), L-870,810 (23), and S-1360 (16) were synthesized as described previously. The structures of EVG and L-870,810 are depicted in Fig. 1.

Cells and viruses. MT-2 and MT-4 cells were grown in RPMI 1640 medium. 293T cells were grown in Dulbecco's modified Eagle's medium. These media were supplemented with 10% fetal calf serum, 2 mM L-glutamine, 100 U/ml penicillin, and 50 μg/ml streptomycin. HeLa-CD4/CCR5-LTR/β-gal cells (5) were kindly provided by J. Overbaugh through the AIDS Research and Reference Reagent Program, Division of AIDS, National Institute of Allergy and Infectious Diseases (Bethesda, MD), and maintained in Dulbecco's modified Eagle's medium supplemented with 10% fetal calf serum, 200 μg/ml hygromycin B, 10 μg/ml puromycin, and 200 μg/ml geneticin. Peripheral blood mononuclear cells (PBMC) were obtained from healthy HIV-1-seronegative donors by centrifugation through Ficoll-Hypaque density gradients. PBMC were stimulated with 20 U/ml interleukin-2 (Shionogi, Osaka, Japan) and 0.5 μg/ml phytohemagglutinin (Sigma) for 3 days and then used for assays as described previously (30).

Three laboratory strains, HIV-1_{IIIB}, HIV-2_{EHO}, and HIV-2_{ROD}, were used in this study. Various subtypes of drug-naïve clinical isolates of HIV-1 (four isolates of subtype B and seven isolates of non-B subtypes) were employed. Four drug-resistant clinical isolates of HIV-1, including IVR401, IVR409, IVR411, and IVR415, were kindly provided by S. Oka (AIDS Clinical Center, International Medical Center of Japan, Tokyo, Japan).

Determination of HIV drug susceptibility. Inhibitory effects of compounds on HIV infection were determined using multinuclear activation of a galactosidase indicator (MAGI) assay, as previously described (37). Inhibitory effects on HIV-1 clinical isolates were measured by p24 production, and cytotoxicity was measured by using a 3-(4,5-dimethylthiazol-2-yl)-2,5-diphenyltetrazolium bromide (MTT) colorimetric assay, as described previously (30). Antiviral activities and cytotoxicities of inhibitors are presented as the concentrations that block viral replication by 50% (50% effective concentration [EC_{50}]) and that suppress the viability of target cells by 50%, respectively.

Quantification of HIV-1 DNA species. MT-2 cells (5×10^5 cells) were infected with HIV-1_{IIIB} at a multiplicity of infection (MOI) of 0.1 in the absence or presence of various inhibitors. Infected cells were washed after incubation for 2 h at 37°C. At 24 h postinfection, DNA was extracted using DNAzol reagent (Invitrogen, Carlsbad, CA).

Quantification of integrated HIV-1 DNA and the two-long-terminal-repeat (2-LTR) circle was performed by real-time quantitative PCR as described previously (4). To normalize DNA species among inhibitors, β-globin amplification was used as an internal control (51). Reactions were analyzed by using the ABI Prism 7500 sequence detector (PE Applied Biosystems, Foster City, CA), and results were then normalized and expressed as relative HIV-1 DNA species compared to a "no-inhibitor" control.

In vitro strand transfer assay. An oligonucleotide-based strand transfer assay was performed as previously described (8), with some modifications. Briefly, preprocessed oligonucleotide H-U5V1-2 (5′-ATGTGGAAAATCTCTAGCA-3′), derived from the U5 end of the HIV-1 LTR, was labeled at the 5′ end with [γ-^{32}P]ATP. Radiolabeled H-U5V1-2 was annealed to H-U5V2 (5′-ACTGCTA GAGATTTTCCACAT-3′) and then used for assays. Recombinant HIV-1 IN derived from HIV-1 NL4-3 (wild type) or EVG-selected mutants was prepared using an *Escherichia coli* expression system. The strand transfer assay was performed with 1 μM IN and 150 nM substrate DNA in 20 mM MOPS (morpholinepropanesulfonic acid) buffer with 30 mM $MgCl_2$ incubated in either the presence or absence of IN inhibitors at 37°C for 60 min. Reaction products were analyzed by electrophoresis on 25% polyacrylamide gels and quantified using a BAS-2500 imaging system (Fuji Photo Film, Tokyo, Japan). The concentration of IN inhibitor that inhibited the production of strand transfer products by 50% (50% inhibitory concentration [IC_{50}]) compared to the control was determined.

Selection of EVG-resistant HIV-1 variants in vitro. MT-2 cells (2×10^5 cells) were infected with HIV-1_{IIIB} and then cultured in the presence of 0.5 nM (see Fig. 3A) or 0.1 nM (see Fig. 3B) EVG. Cultures were incubated at 37°C until an

TABLE 1. Antiviral activities against laboratory HIV strains[a]

Strain	Mean EC_{50} (nM) ± SD		
	AZT	EVG	L-870,810
$HIV\text{-}1_{IIIB}$	7.1 ± 1.3	0.7 ± 0.3	6.3 ± 0.3
$HIV\text{-}2_{EHO}$	22 ± 9.1	2.8 ± 0.8	11 ± 1.9
$HIV\text{-}2_{ROD}$	19 ± 4.7	1.4 ± 0.7	8.6 ± 0.4

[a] Antiviral activity was determined using the MAGI assay. Data shown are means and standard deviations obtained from at least three independent experiments.

extensive cytopathic effect (CPE) was observed, and the culture supernatant was then harvested for further passage in fresh MT-2 cells. The concentration of EVG was increased when a significant CPE was observed. At the indicated passages (see Fig. 3A and B), proviral DNA was extracted from infected MT-2 cells and then subjected to PCR, followed by direct population-based sequencing. Susceptibility to EVG at the indicated passages was determined using the MAGI assay (see Fig. 3A) or p24 production (see Fig. 3B).

Recombinant HIV-1 clones. An HIV-1 infectious clone, pNL101 (38), kindly provided by K.-T. Jeang (NIH, Bethesda, MD), was used to generate recombinant HIV-1 clones. Wild-type HIV-1 ($HIV\text{-}1_{WT}$) was constructed by replacing the *pol* coding region (nucleotide positions 2006 of the ApaI site to 5122 of the NdeI site of pNL101) with HIV-1 strain BH10. The *pol* coding region contains a silent mutation at nucleotide 4232 (TTTAGA to TCTAGA) resulting in the generation of a unique XbaI site. Recombinant HIV-1 IN infectious clones were generated using a modified pNL101-based vector, $pNLRT_{WT}$. In brief, mutations were introduced into the XbaI-NdeI region (891 bp) of $pSLInt_{WT}$, which encodes nucleotides 4232 to 5122 of pNL101, using an oligonucleotide-based site-directed mutagenesis method (54). Next, the XbaI-NdeI fragments were inserted into pBNΔInt, which encodes nucleotides 5122 (NdeI) to 5785 (SalI) of pNL101. Finally, the XbaI-SalI region (1,554 bp) was inserted into pNL101. Each infectious clone was transfected into 293T cells. The following day, MT-2 cells were added, and the supernatants were harvested when an extensive CPE was observed.

Replication kinetics of resistant HIV-1 variants. MT-2 cells (10^5 cells) were infected with each virus preparation (500 MAGI units) for 4 h. The infected cells were then washed and cultured in the presence or absence of EVG. The culture supernatants were harvested on day 5 after infection, and p24 levels were quantified using a Retro-Tek HIV-1 p24 antigen enzyme-linked immunosorbent assay (ELISA) (ZeptoMetrix, Buffalo, NY).

Evaluation of antiretroviral activities of IN inhibitors. The MLV-based retroviral vector pRCV/LIG (15) and plasmid pcDNA-VSVG, encoding the vesicular stomatitis virus envelope glycoprotein (a generous gift from H. Miyoshi, RIKEN Bioresource Center, Tsukuba, Japan), were employed to generate viral particles. These plasmids were cotransfected into an MLV-derived Gag-Pol-expressing packaging cell line, GP293 (Clontech, Palo Alto, CA). After 48 h of transfection, culture supernatants were filtered through a 0.45-μm membrane and stored at −80°C until use.

An HIV-1-based luciferase expression vector, pBC-LIG; pCMVΔ8/9, encoding the HIV-1 viral proteins including IN; and pcDNA-VSVG were transfected into 293T cells to generate pseudotyped HIV-1. The viruses were used to infect 293T cells (10^5 cells per well in 12-well plates) at an MOI of 0.02 in the absence or presence of inhibitors. After 48 h of transduction, luciferase activity was determined using a luciferase assay system (Promega, Madison, WI) and an LB 9507 luminometer (Berthold, Bad Wildbad, Germany).

An SIV molecular clone, pMA239 (46), containing the full SIVmac239 genome, was a kind gift from E. Ido, Institute for Virus Research, Kyoto University. pMA239 was used to generate viral stocks as previously described (6). Antiviral activities of IN inhibitors against SIVmac239 were determined using the MAGI assay as described above.

Molecular modeling studies. A three-dimensional model of EVG in complex with HIV-1 IN CCD was prepared by PyMOL software, version 0.97, using previously reported data (44). Amino acid residues involved in resistance to EVG were displayed within this model.

RESULTS

Anti-HIV activities of IN inhibitors. The antiviral activity of EVG against $HIV\text{-}1_{IIIB}$, $HIV\text{-}2_{EHO}$, and $HIV\text{-}2_{ROD}$ was first evaluated by the MAGI assay. EVG showed potent antiviral activity against three laboratory strains of HIV, with EC_{50} values in the subnanomolar to nanomolar range (Table 1). Next, we evaluated the activity of EVG against wild-type clinical isolates representing various subtypes of HIV-1. EVG suppressed the replication of all HIV-1 subtypes tested, with an antiviral EC_{50} ranging from 0.10 to 1.26 nM (Table 2). Moreover, EVG suppressed the replication of HIV-1 clinical isolates carrying NRTI, NNRTI, and PI resistance-associated genotypes, as did a control IN inhibitor, the compound L-870,810 (see Table S1 in the supplemental material). The cytotoxicities of these inhibitors were also determined using an MTT colorimetric assay. Mean values for the concentration that suppresses the viability of target cells by 50% for EVG and L-870,810 in PBMC obtained from three independent donors were 4.6 ± 0.5 μM and 2.7 ± 0.6 μM, respectively. Thus, EVG can suppress various HIV strains, including diverse HIV-1 subtypes and clinical isolates carrying multiple mutations associated with resistance to currently approved antiretroviral drugs.

TABLE 2. Antiviral activities of EVG against various subtypes of HIV-1[a]

Subtype	Isolate	EC_{50} (nM)	
		AZT	EVG
A	RW/92/016	7.91	0.41
B	96USHIPS7	8.41	0.26
	BR/92/021	2.13	0.76
	BR/93/017	1.10	0.18
	BR/93/022	11.7	1.13
C	BR/92/025	2.84	0.10
D	UG/92/046	7.26	0.50
E	CMU02	9.07	1.26
F	BR/93/020	25.3	0.74
G	JV1083	11.1	0.35
O	BCF01	1.52	1.17

[a] Antiviral activity was determined using p24 ELISA.

Mechanism of anti-HIV activity of EVG. First, we performed a "time-of-addition" experiment as described previously (30), with some modifications. MT-4 cells were infected with $HIV\text{-}1_{IIIB}$ at an MOI of 0.5. One hour after infection, infected cells were extensively washed, and compounds were added, including an NNRTI (EFV at 100 nM), a PI (NFV at 500 nM), or EVG (100 nM). Amounts of p24 antigen were determined at 31 h postinfection. The antiviral activity of EFV gradually decreased from 6 h postinfection and disappeared at 12 h postinfection, whereas the antiviral activity of EVG decreased from 10 h postinfection and was no longer detected by 12 h postinfection. On the other hand, the PI NFV effectively blocked the infection up to 12 h postinfection and still exerted approximately 20% inhibitory activity up to 24 h postinfection. These results strongly suggest that EVG inhibits the HIV replication at a step that occurs after reverse transcription but before proteolytic cleavage, consistent with the integration step.

To elucidate the mode of action of EVG on HIV-1 replication, the levels of intracellular HIV-1 DNA species were determined using real-time quantitative PCR (Fig. 2A). MT-2 cells were infected with $HIV\text{-}1_{IIIB}$ in the presence or absence

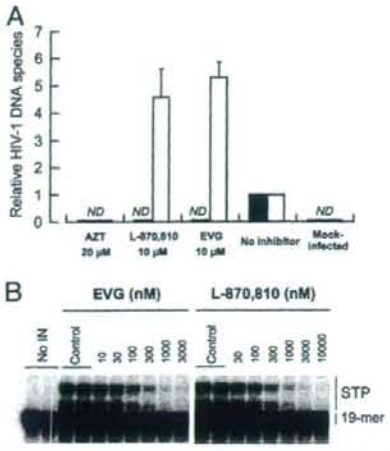

FIG. 2. Mechanism of action of EVG. (A) Quantification of HIV-1 DNA species. MT-2 cells were infected with HIV-1_{IIIB} in the presence or absence of AZT, L-870,810, and EVG. Unintegrated (2-LTR) (white bars) and integrated (black bars) forms of proviral DNA were quantified by real-time PCR and normalized to the β-globin gene after 24 h of infection. The data are represented as means and standard deviations of value relative to that of the no-inhibitor control from three independent experiments. ND means that the signals were not detected even after 40 cycles of amplification. (B) Inhibitory effect of IN inhibitors on strand transfer activity. Gel electrophoresis shows strand transfer products (STP) generated from preprocessed donor DNA substrate (19-mer) covalently bound to acceptor DNA.

of a CD4-gp120 binding inhibitor, DS5000; an NRTI, AZT; an IN inhibitor, L-870,810; and EVG. Unintegrated (2-LTR) and integrated forms of reverse-transcribed HIV-1 genomic DNA were quantified after 24 h of infection and then normalized with β-globin DNA. In the presence of 20 μM AZT, neither 2-LTR nor integrated forms were detected as expected. Similar results were also observed with 20 μM DS5000 (data not shown). In the presence of 10 μM L-870,810, integrated provirus was undetectable, while relative 2-LTR levels increased about 5-fold (4.6-fold ± 1.0-fold). Similar results were observed with 10 μM EVG (2-LTR) (5.3-fold ± 0.5-fold), indicating that EVG exerts anti-HIV activity by blocking the integration step.

To further characterize the mechanism by which EVG inhibits the integration step, the effect of EVG on strand transfer was assessed by characterizing its ability to inhibit the activity of recombinant wild-type HIV-1 IN enzyme in an oligonucleotide-based strand transfer assay (Fig. 2B). EVG and L-870,810 both inhibited the synthesis of strand transfer products with IC_{50} values of 54 nM and 118 nM, respectively. Taken together, these results indicate that like L-870,810, EVG blocks integration via the inhibition of IN-mediated strand transfer.

Selection of EVG-resistant HIV-1 variants in vitro. To determine the in vitro resistance profile of EVG, EVG-resistant viral variants were selected using a dose escalation method, and the susceptibilities of the resulting selected variants to EVG (EC_{50}) were determined. Selection of resistant HIV-1_{IIIB} was initiated with 0.5 nM EVG (Fig. 3A). At passage 12 (P-12), where the concentration of EVG was 4 nM, 2 amino acid substitutions, glutamine-to-proline at IN codon 146 (Q146P) and asparagine-to-aspartic acid at IN codon 232 (N232D), were observed (Fig. 3A). An N232D substitution was previously reported to be an IN polymorphism in HIV-1 (34). The EVG EC_{50} of a P-24 variant containing a Q146P- and N232D-substituted variant was 6.2 nM. At P-32 (32 nM EVG), a T66I IN substitution was newly observed, whereas the N232D substitution had reverted to the baseline sequence. The EVG EC_{50} against a P-36 variant was 64 nM. An S147G IN substitution was detected at P-48 (128 nM EVG), and the EVG EC_{50} further increased to 635 nM. In addition, a Q95Q/K IN substitution (mixture of Q and K) and an E138E/K IN substitution were newly identified at P-54 (256 nM EVG). These mixtures, Q95Q/K and E138E/K, fully emerged in the viral pools by P-64 and P-80, respectively. The EVG EC_{50} at P-68 (1,024 nM EVG) was greater than 1,000 nM.

An independent EVG selection experiment, again using HIV-1_{IIIB}, was performed but began at 0.1 nM EVG (Fig. 3B). An E92E/Q mixture in the IN coding region was first detected at P-30 (10 nM EVG) and was predominantly E92Q by P-38 (20 nM EVG). Additional IN substitutions, H51H/Y and S147S/G, emerged at P-60 (640 nM EVG), and an E157E/Q mixture emerged at P-70 (1,280 nM EVG); the viral pools at the terminal passage P-80 (1,280 nM EVG) had the IN sequence H51Y/E92Q/S147G/E157E/Q (Fig. 3B). The emergence of each of these mutations correlated with an increase in the EVG EC_{50} of the resulting viral pools (Fig. 3). Other than the N232D polymorphism, all of these mutations are located in the CCD of IN.

Phenotypic analysis of IN recombinant viruses. (i) EVG-selected mutations. To characterize which mutations are responsible for EVG resistance, infectious HIV-1 clones containing single IN substitutions (H51Y, T66I, E92Q, Q95K, E138K, Q146P, S147G, or E157Q) that were observed to emerge under selection with EVG were generated (Fig. 3 and Table 3). Mutations were classified into two groups based on the level of resistance: mutations that conferred more than 10-fold reduced susceptibility compared to the wild type were defined as primary mutations, and mutations conferring less than 10-fold reduced susceptibility were defined as secondary mutations. T66I and E92Q substitutions conferred significantly reduced susceptibility to EVG (37- and 36-fold reduced, respectively, relative to the wild type), whereas the Q146P and S147G substitutions conferred more moderate reductions in EVG susceptibility (11-fold reduced), indicating that these four IN mutations are primary mutations involved in resistance to EVG. In contrast, H51Y, Q95K, and E157Q substitutions all conferred smaller reductions in EVG susceptibility (each less than 6.3-fold reduced compared to the wild type), suggesting that these substitutions are secondary resistance mutations. Interestingly, the E138K mutation alone conferred no reduction in susceptibility to either EVG or L-870,810. Thus, several distinct mechanisms of resistance may be represented by these different IN mutations.

Multisubstituted clones observed during EVG selection experiments were also generated. HIV-$1_{T66I/Q146P}$ showed high-level resistance to EVG (119-fold reduced susceptibility) (Table 3). Combinations of S147G with T66I/Q146P or E92Q further enhanced resistance, 412- and 356-fold, respectively.

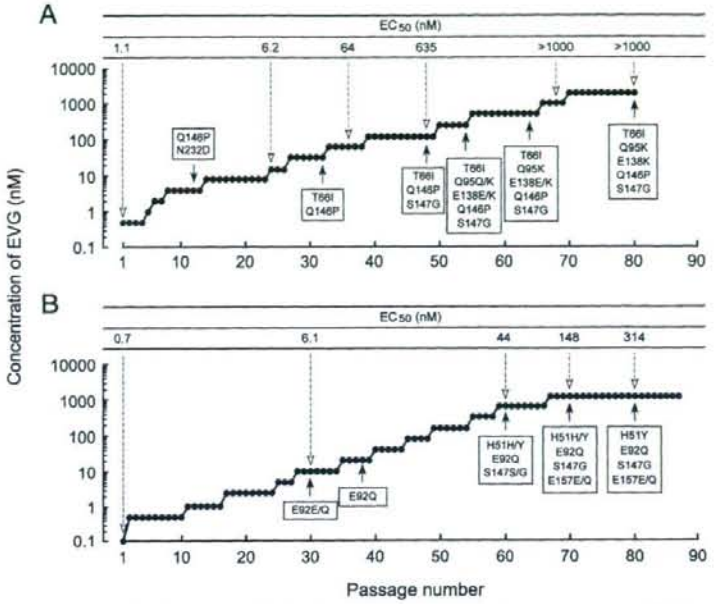

FIG. 3. Induction of EVG-resistant HIV-1. Data from MT-2 cells are shown. The initial concentrations of EVG were 0.5 nM (A) and 0.1 nM (B). Results are from two identical but independent experiments. At the indicated passage number (black arrowheads), proviral DNA extracted from infected MT-2 cells was sequenced. Amino acid substitutions are shown. The EC_{50} values of HIV-1 variants selected by EVG at the indicated passage number (white arrowheads) were determined using MAGI assay (A) or the production of p24 in MT-2 cells (B).

The triple mutant HIV-$1_{H51Y/E92Q/S147G}$ showed high-level resistance to EVG (700-fold reduced susceptibility). Interestingly, the addition of the secondary mutation H51Y, which on its own reduced EVG susceptibility only 3.6-fold, substantially enhanced resistance relative to that observed for the double mutant HIV-$1_{E92Q/S147G}$. HIV-$1_{T66I/Q95K/Q146P/S147G}$, HIV-$1_{T66I/Q95K/E138K/Q146P/S147G}$, and HIV-$1_{H51Y/E92Q/S147G/E157Q}$ mutants all showed high-level resistance to EVG, with EC_{50} values greater than 1,000 nM in all cases. These results indicate that the T66I and E92Q mutations provided the highest change (*n*-fold) in EVG susceptibility as individual resistance mutations and that the additional substitutions identified further enhance the level of resistance to EVG when combined with these primary mutations.

(ii) L-870,810-selected mutations. Infectious HIV-1 clones containing mutations (V72I, F121Y, T125K, and V151I) previously shown to be associated with resistance to L-870,810 (23) and two mutations, L74M and G163R, observed in our selection using L-870,810 (data not shown) were generated. Among these variants, HIV-1_{F121Y} and HIV-1_{V151I} demonstrated reduced susceptibility to both L-870,810 and EVG (Table 3). V151I has been observed in some HIV-1 clinical isolates and may be an IN polymorphism (34). Moreover, the effect of V151I on susceptibility to L-870,810 has been controversial (23, 29). This discrepancy might arise from the viral strain or plasmid backbone used, so further experiments to clarify the effect of V151I on IN inhibitor susceptibility are needed. HIV-$1_{F121Y/T125K}$ showed significant resistance to both L-870,810 and EVG (68-fold and 177-fold reduced susceptibility, respectively). HIV-$1_{V72I/F121Y/T125K/V151I}$ showed high-level resistance to both IN inhibitors (EC_{50} greater than 1,000 nM).

(iii) DKA IN inhibitor-selected mutations. Highlighting the potential for related mechanisms of IN inhibitor resistance and cross-resistance, the T66I mutation has also been observed to be selected by DKA IN inhibitors such as L-708,906 and S-1360. Additional mutations, L74M and S153Y, in combination with T66I were also observed to be selected by these DKA IN inhibitors (16, 17). L74M also emerged during L-870,810 selection in our studies (data not shown) but conferred no change in susceptibility to L-870,810 when present alone and only low-level resistance (3.0-fold) to EVG (Table 3). The combination of T66I and L74M conferred slightly higher resistance to EVG (45-fold) than did T66I alone but only moderate resistance to L-870,810 (7.1-fold). Another IN mutant, HIV-$1_{T66I/S153Y}$, observed in L-708,906 selection experiments (24) showed high-level resistance to EVG (260-fold) but low-level resistance to L-870,810 (5.0-fold). These results suggest that the mechanism of EVG resistance may have some similarities to that of DKA IN inhibitors.

Taken together, these results suggest that a variety of IN mutations may be selected by EVG and other IN inhibitors. Most of the IN inhibitor resistance mutations are observed to cluster in the CCD of IN. The resulting mutations and their combinations have the capacity to confer various levels of resistance and potential cross-resistance to EVG and other IN inhibitors. Given their location in the CCD, many of these mutations may act via a common mechanism. The observed development of IN inhibitor resistance mutations resembles

TABLE 3. Susceptibilities of HIV-1 IN recombinant molecular clones[a]

Molecular clone(s)	Mean EC_{50} (nM) ± SD (fold resistance compared to wild type)				
	AZT	EVG	L-870,810	S-1360	L-731,988
$HIV\text{-}1_{WT}$	32	1.1	5.8	1,239	736
EVG mutation (expt 1)[b]					
T66I[c]	43 ± 11 (1.3)	41 ± 14 (37)	4.7 ± 2.9 (0.8)	6,403 ± 2,349 (5.2)	7,234 ± 1,210 (9.8)
Q95K	34 ± 6 (1.1)	2.9 ± 0.4 (2.6)	18 ± 2 (3.1)	ND	ND
E138K	33 ± 8 (1.0)	1.1 ± 0.4 (1.0)	3.9 ± 0.4 (0.7)	ND	ND
Q146P	26 ± 2 (0.8)	12 ± 3 (11)	5.1 ± 0.4 (0.9)	ND	ND
S147G[d]	41 ± 5 (1.3)	12 ± 5 (11)	23 ± 6 (4.0)	ND	ND
T66I/Q146P	22 ± 2 (0.7)	131 ± 12 (119)	18 ± 5 (3.1)	ND	ND
T66I/Q146P/S147G	19 ± 5 (0.6)	453 ± 62 (412)	127 ± 37 (22)	ND	ND
T66I/Q95K/Q146P/S147G	31 ± 12 (1.0)	>1,000	303 ± 76 (52)	ND	ND
T66I/Q95K/E138K/Q146P/S147G	41 ± 7 (1.3)	>1,000	306 ± 76 (53)	>10,000	>50,000
EVG mutation (expt 2)[b]					
H51Y	34 ± 8 (1.1)	4.0 ± 0.6 (3.6)	3.3 ± 0.7 (0.6)	ND	ND
E92Q	32 ± 4 (1.0)	40 ± 12 (36)	63 ± 39 (11)	ND	ND
E157Q	34 ± 8 (1.1)	6.9 ± 1.4 (6.3)	52 ± 20 (9.0)	ND	ND
E92Q/S147G	39 ± 9 (1.2)	392 ± 133 (356)	587 ± 64 (101)	ND	ND
H51Y/E92Q/S147G	54 ± 6 (1.7)	769 ± 88 (699)	374 ± 100 (64)	>10,000	22,175 ± 1,299 (30)
H51Y/E92Q/S147G/E157Q	21 ± 2 (0.7)	>1,000	340 ± 26 (59)	>10,000	18,652 ± 4,575 (25)
L-870,810 mutation					
V72I	17 ± 1 (0.5)	4.3 ± 1.1 (3.9)	9.1 ± 2.5 (1.6)	ND	ND
L74M[c]	20 ± 3 (0.6)	3.3 ± 1.1 (3.0)	4.4 ± 1.7 (0.8)	1,500 ± 302 (1.2)	4,471 ± 942 (6.1)
F121Y	15 ± 1 (0.5)	28 ± 11 (25)	51 ± 23 (8.8)	ND	ND
T125K	17 ± 3 (0.5)	2.3 ± 1.1 (2.1)	9.9 ± 3.7 (1.7)	ND	ND
V151I	21 ± 4 (0.7)	11 ± 3 (10)	104 ± 29 (18)	ND	ND
G163R	22 ± 7 (0.7)	0.8 ± 0.2 (0.7)	6.5 ± 2.6 (1.1)	ND	ND
F121Y/G163R	36 ± 5 (1.1)	60 ± 20 (55)	219 ± 20 (38)	ND	ND
F121Y/T125K	38 ± 12 (1.2)	195 ± 73 (177)	393 ± 82 (68)	ND	ND
V72I/F121Y/T125K	33 ± 7 (1.0)	143 ± 25 (130)	886 ± 79 (153)	ND	ND
V72I/F121Y/T125K/V151I	64 ± 9 (2.0)	>1,000	>1,000	>10,000	>50,000
DKA mutation					
T66I/L74M	46 ± 11 (1.4)	49 ± 5 (45)	41 ± 10 (7.1)	>10,000	23,043 ± 4,886 (31)
T66I/S153Y	26 ± 8 (0.8)	285 ± 63 (259)	29 ± 9 (5.0)	>10,000	8,478 ± 1,267 (12)

[a] Antiviral activity was determined using the MAGI assay. Data shown are means and standard deviations obtained from at least three independent experiments, and resistance (*n*-fold) of the EC_{50} of the IN recombinant molecular clone compared to that of parental $HIV\text{-}1_{WT}$ is shown in parentheses. ND, not determined.
[b] EVG selection was performed in two independent experiments, and observed mutations are separately represented.
[c] Also observed in the DKA selected mutation.
[d] Observed in two independent EVG-selected experiments.

that seen for other antiretroviral drugs such as PIs; i.e., multiple mutations are introduced in a stepwise fashion and are required for high-level resistance to the selecting inhibitors (10, 50).

Strand transfer assay. To further characterize the effect of EVG-selected resistance mutations on IN function, the effect of mutations on the enzymatic activity of recombinant IN was evaluated in an in vitro strand transfer assay (Fig. 4). IN enzymes carrying the individual mutations H51Y, S147G, and E157Q had reduced strand transfer activity relative to that of the wild type (57%, 36%, and 79% of wild-type levels, respectively). Strand transfer activities of E92Q, E92Q/S147G, and H51Y/E92Q/S147G IN enzymes decreased with the accumulation of mutations from 57% to 29 and 22% of the wild type, respectively. However, the introduction of E157Q to H51Y/E92Q/S147Q partially restored strand transfer activity to 46% of wild-type activity, suggesting that E157Q may play a role in compensating for the loss of strand transfer activity resulting from the emergence of EVG resistance mutations.

The effect of EVG-selected mutations on the inhibition of strand transfer by EVG and L-870,810 was also determined (Fig. 4). Recombinant IN enzymes carrying the individual H51Y, S147G, and E157Q substitutions remained susceptible to both EVG and L-870,810 (0.7- to 2.1-fold reduced susceptibility). E92Q IN demonstrated only moderate resistance to both IN inhibitors in the strand transfer assay (4.3-fold reduced for both inhibitors). The combination of E92Q and S147G enhanced resistance to both EVG and L-870,810 (7.6- and 8.5-fold reduced susceptibility, respectively). However, unlike the IN recombinant viruses in the antiviral assay, neither the H51Y/E92Q/S147G nor the H51Y/E92Q/S147G/E157Q IN enzymes showed further enhancement of resistance in the strand transfer assay. This difference in results from the strand transfer assay versus those from the antiviral assay may reflect differences in the recombinant IN enzyme versus the viral IN enzyme in situ. Indeed, structure-activity relationship experiments described in a previous report (43) revealed that antiviral activity and in vitro enzyme inhibition were well correlated. Nevertheless, this biochemical analysis confirmed that the E92Q IN mutation confers significantly reduced suscepti-